

AERE R 12405

APPROVED FOR PUBLICATION

AERE R 12405

THIS DOCUMENT IS INTENDED FOR PUBLICATION IN THE OPEN LITERATURE.
Until it is published, it may not be circulated, or referred to outside the organisation to
which copies have been sent.

1

AD-A190 091

DTIC FILE COPY

United Kingdom Atomic Energy Authority

HARWELL

DTIC
ELECTE
S JAN 1 1 1988 D
D

**Diffusion in oxides of the first
transition series metals**

A Atkinson

DISTRIBUTION STATEMENT A
Approved for public release;
Distribution Unlimited

COPYRIGHT AND REPRODUCTION
Enquiries about copyright and reproduction should be addressed to the
Publications Office, AERE Harwell, Oxfordshire, England OX11 0RA

Materials Development Division
Harwell Laboratory, Oxfordshire OX11 0RA

December 1986

APPROVED FOR PUBLICATION

87 12 00 07 5

DIFFUSION IN OXIDES OF THE FIRST TRANSITION SERIES METALS

A Atkinson

ABSTRACT

The elements of the first transition series form oxides which display a wide variety of defect-related phenomena such as non-stoichiometry and diffusion. Many of these oxides have been studied extensively in recent years; partly because of their intrinsic interest and partly because they are important technologically (e.g. in high temperature oxidation, catalysis etc.).

In this paper the current appreciation of diffusion processes in some of these oxides is reviewed in terms of the defects which are believed to be responsible for diffusion and their energies of formation, migration and interaction. Particular emphasis is given to the large contribution made to this field by N L Peterson and his co-workers.

The specific materials considered are TiO_2 , Cr_2O_3 , MnO , FeO , Fe_3O_4 , Fe_2O_3 , CoO , NiO and Cu_2O .

Materials Development Division
Harwell Laboratory

December 1986

HL86/1478 (C14)

For	<input checked="" type="checkbox"/>
General	<input type="checkbox"/>
Special	<input type="checkbox"/>
Priority Codes	
Special	
A-1	

CONTENTS

	<u>Page No.</u>
1. Introduction	1
2. Theoretical background	2
3. TiO_2 (rutile)	4
3.1 Self diffusion in TiO_2	4
3.2 Impurity diffusion in TiO_2	6
4. NiO, CoO, MnO and FeO	6
4.1 Point defects and cation self diffusion	7
4.2 Oxygen self diffusion	10
4.3 Behaviour of impurities	12
5. Fe_3O_4 (magnetite)	14
6. Fe_2O_3 (hematite) and Cr_2O_3 (chromite)	15
6.1 Fe_2O_3	15
6.2 Cr_2O_3	17
7. Cu_2O (cuprite)	19
8. Diffusion along grain boundaries and dislocations	20
9. Concluding remarks	21
Acknowledgement	23
References	24

TABLES

Table

1 Defect parameters for TiO_2	29
2 Experimental defect parameters for NiO, CoO and MnO	30
3 Calculated point defect energies (eV) for NiO	31
4 Point defect parameters for Cu_2O [62]	32

ILLUSTRATIONS

- Fig. 1 The crystal structure of TiO_2 (rutile) viewed parallel to the c axis. One of the channels containing potential interstitial sites is indicated.
- Fig. 2 Tracer diffusion of Co, Fe, Ti and Sc parallel to the c direction in TiO_2 as a function of a_{O_2} at 1100°C - 1000°C for Fe). The indicated slopes of $n = -0.25$ and $n = -0.20$ correspond to Ti_1^3 and Ti_1^4 defects respectively (refs. 6, 12 and 13).
- Fig. 3 Schematic diagram indicating how fast diffusion of certain impurities along the c-direction in TiO_2 probably occurs by a mixture of interstitialcy and direct interstitial jumps.
- Fig. 4 Comparison between the measured and calculated enthalpies of motion for cation vacancy self-diffusion in the rocksalt oxides.
- Fig. 5 Arrhenius plots at constant a_{O_2} (except for FeO) of oxygen tracer self-diffusion in the rocksalt oxides (refs. 30-33).
- Fig. 6 The dependence of oxygen tracer coefficient on oxygen activity in FeO and CoO (refs. 31 and 34).
- Fig. 7 Arrhenius plot of the diffusion coefficient of iron vacancies and interstitials in Fe_3O_4 . The extent of uncertainty is partly due to experiment and partly due to the range of possible correlation factors which are consistent with the experiments (ref. 24).
- Fig. 8 Arrhenius plot at constant a_{O_2} ($= 1$) of the tracer diffusion coefficient of Fe parallel to the c-direction in Fe_2O_3 . The two data sets of Hoshino and Peterson are for crystals from different sources (refs. 51-53).
- Fig. 9 The thermoelectric power of sintered Cr_2O_3 as a function of a_{O_2} . The n to p transition is complete within 7 days at 1247°C , but the reverse transition will not take place unless the temperature is raised to 1500°C (ref. 58).
- Fig. 10 Tracer diffusion of Cr parallel to the c-direction in Cr_2O_3 as a function of a_{O_2} . The indicated values of $n = +0.188$ or $n = -0.188$ are expected for diffusion by vacancies or interstitials respectively according to the simple defect model (refs. 60 and 61).
- Fig. 11 Tracer diffusion of Cu and oxygen in Cu_2O as a function of oxygen activity. The indicated slopes are for a simple model in which Cu diffuses by singly charged vacancies and oxygen by singly charged interstitials (refs. 62 and 63).
- Fig. 12 Tracer diffusion of Ni and O in the lattice, along dislocations and along grain boundaries in NiO . $a_{\text{C}_2} = 1$ for Ni and 0.2 for O (refs. 68, 69 and 70).

1. Introduction

The oxides of the first transition series metals exhibit a wide range of interesting properties e.g. electronic, magnetic, chemical etc. They have therefore been studied widely; sometimes because they have technologically useful properties (e.g. fast ion conductors, catalysts, corrosion resistant barriers) and sometimes because they are of fundamental interest. The interesting properties have their origin in the unfilled electronic 3d shell of the metal ion. The relative ease with which electrons can be removed or added to some of these ions means that they can often exist in a number of valence states giving rise to a potentially large number of oxide phases which themselves deviate from exact stoichiometry by an amount depending on the thermodynamic activity of oxygen with which they are equilibrated, a_{O_2} . The deviation from stoichiometry has a large influence on diffusion in such oxides and it is the relationship between the two which is the subject of this review. Since it is this relationship, expressed in terms of crystal defects, which is at the heart of understanding diffusion, the experiments which are of most direct interest are measurements of deviation from stoichiometry and tracer diffusion coefficients; particularly as a function of a_{O_2} . These are supported, however, by other less direct measurements which are also related to the crystal defects and their motion such as isotope effect, electrical conductivity, thermoelectric power and chemical diffusion. In a straightforward ideal case all such experiments may be rationalised in terms of a model for the point defect populations in the crystal, characterised by parameters describing their energies of formation and motion which are in agreement with theoretical predictions based on atomistic calculations. This goal has not yet been realised for a transition metal oxide.

The range of materials covered in this review has been restricted to only a small representative selection of the large number potentially encompassed by the title. Those included are TiO_2 , Cr_2O_3 , MnO , FeO , Fe_3O_4 , Fe_2O_3 , CoO , NiO and Cu_2O . For each oxide the current understanding of its defect structure and diffusion properties will be summarised and attention drawn to those aspects which are unresolved or

inconsistent. Finally, we briefly consider fast diffusion along dislocations and grain boundaries.

2. Theoretical background

The theoretical treatment of point defects in ionic crystals has been summarised by Lidiard [1] and Kröger [2]. A survey of the application of these ideas to oxides up to 1972 has been given by Kofstad [3]. The approach, which has now become standard in the field, is to write defect reactions in an analogous way to chemical reactions and apply 'mass action laws' to relate their concentrations at equilibrium. In the case of transition metal oxides the oxidation/reduction reactions tend to dominate and it is therefore convenient to write the defect formation reactions in that form. An example of an oxidation reaction for an oxide MO is



and of a reduction reaction



In this paper the free energy change of such reactions will be referred to as the energy of formation of the appropriate lattice defect, g_f . The mass action equations corresponding to these reactions are strictly written in terms of chemical activities of the defects (e.g. $\{V_M^{''}\}$) but these are usually approximated by the defect concentration expressed as a molecular fraction (e.g. $[V_M^{''}]$) of the oxide assumed to have its conventional stoichiometric formula. The equilibrium constant for the defect-forming reaction is then related to the standard free energy of formation by

$$g_f = h_f - Ts_f = -kT \ln K$$

In an isotropic lattice, the tracer diffusion coefficient, D^* , is given by [1]

$$D^* = \frac{1}{6} f \Gamma r^2 \quad (4)$$

where Γ is the jump frequency and r the jump distance. f is the correlation factor which accounts for the non-random motion of the tracer and is characteristic of the lattice and diffusion mechanism. For a vacancy mechanism in an fcc or bcc lattice of lattice constant a_0 , equation (4) becomes

$$D^* = a_0^2 w_0 f \quad (5)$$

where w_0 is the rate of exchange between a vacancy and a neighbouring ion. Hence the diffusion coefficient of the vacancy is

$$D_v = a_0^2 w_0$$

Since the jump is thermally activated over a free energy barrier the jump frequency is related to the vibrational frequency ν by

$$w_0 = \nu \exp(s_{\square}/k) \exp(-h_{\square}/kT) \quad (6)$$

where s_{\square} and h_{\square} are the entropy and enthalpy of motion of the defect.

Application of mass action to reactions such as (1) and (2) when combined with the condition for overall electrical neutrality predicts that defect concentrations are simple functions of oxygen activity of the type

$$[\text{def}] \propto a_{O_2}^n \quad (7)$$

and n is a characteristic of the defect. If only one defect is significant then the deviation from stoichiometry, x , is thus proportional to a_{O_2} to the power n_x . Similarly both electrical conductivity and diffusion are expected to obey such a relationship characterised by exponents n_{σ} and n_D respectively. In practice, this simple behaviour is seldom found which implies the influence of other defects and/or interactions between the dominant defects. The most

common interaction which is invoked is the association of two defects of opposite effective charge on neighbouring sites (e.g. the trapping of a hole near a metal ion vacancy).

Techniques to calculate the characteristic energies of the defects have been developed and applied in some of the oxides discussed here (e.g. Mackrodt [4]). The parameters which are usually calculated are internal energy changes at $T = 0K$ and constant volume which should be approximately equal to enthalpy changes at constant pressure (i.e. h_f and h_m). To enable actual defect concentrations and diffusion rates to be calculated (rather than only their activation energies) techniques are also being developed to estimate the entropy changes, s_f and s_m [5].

3. TiO₂ (rutile)

3.1 Self diffusion in TiO₂

Rutile is oxygen deficient and is conventionally given the formula TiO_{2-x}. This non-stoichiometric rutile is an n-type semiconductor with the dominant defects being titanium interstitials and/or oxygen vacancies. The departure from stoichiometry, x , is very small at $a_{O_2} = 1$, but increases with decreasing a_{O_2} (a typical value being 10^{-2} at $1000^\circ C$ and $a_{O_2} = 10^{-18}$ [3]). Under more reducing conditions extended defects (shear planes) are formed; these will not be discussed here.

Tracer diffusion of Ti in TiO₂ has been studied recently by Hoshino et al [6]. They find that diffusion is typically 50% faster perpendicular to the c axis than parallel to it. (A projection of the rutile structure viewed parallel to the c axis is shown in Fig 1). They also find that D_{Ti}^* behaves in a similar way to x in that it increases as a_{O_2} decreases (Fig 2) which indicates that titanium interstitials are the important defects on the Ti sublattice. Simple defect models in which either $Ti_i^{4\cdot}$ or $V_O^{2\cdot}$ are dominant predict the exponent n in equation 7) for Ti diffusion, n_D , should be -0.20 or -0.33 .

respectively. In practice the experimental results give n close to -0.20 , thus suggesting that $Ti_i^{4\cdot}$ is the defect which is also mainly responsible for nonstoichiometry. However, plots of $\log x$ and $\log \sigma$ versus $\log a_{O_2}$ [3] show distinct curvature and significant deviation from the values $n_x = n_\sigma = -0.20$ which would be expected if only $Ti_i^{4\cdot}$ and compensating electrons need to be considered.

Hoshino et al attempted to rationalise D_{Ti}^* in terms of defect models that had been suggested earlier to account for measurements of x and σ . They specifically tried three models; one with $Ti_i^{3\cdot}$ and $Ti_i^{4\cdot}$, a second with $Ti_i^{4\cdot}$ and $V_O^{2\cdot}$, and a third with $Ti_i^{3\cdot}$, $Ti_i^{4\cdot}$ and $V_O^{2\cdot}$. They found that all three models could be made to fit the data, but the second and third gave zero or negative values of h_m for motion of the interstitial and therefore are not physically acceptable.

Paynaud and Morin [7] have considered some of the pitfalls which may be encountered in fitting defect models to experimental data. They conclude that in the case of TiO_2 the defect $Ti_i^{4\cdot}$ is a necessary feature of an acceptable model; a condition which is satisfied by all three models considered by Hoshino et al. Ait-Younes et al [8,9] concluded from electromigration and chemical diffusion studies that $Ti_i^{3\cdot}$ is the dominant defect in TiO_2 at $1050^\circ C$ which is in agreement with the model favoured by the diffusion studies.

Thus the best model for point defects in TiO_2 appears to be that originally proposed by Blumenthal et al [10] in which $Ti_i^{3\cdot}$ dominate at low temperatures and $Ti_i^{4\cdot}$ at high temperatures. The defect parameters are summarised in Table 1 (the enthalpy of motion for the oxygen vacancy is based on measurements of D_{oxy}^* in impurity-dominated conditions [11]). The structure of TiO_2 (Fig 1) shows channels parallel to the c -axis which could support direct interstitial motion, in which case D_i^* parallel to c would be much greater than D_i^* perpendicular to c . The fact that $D_i^* \ll D_{oxy}^*$ in reality shows that the interstitials move mainly by an interstitial mechanism. From Fig 1 the ratio of displacements

to c and perpendicular to c from an interstitialcy jump is c/a and hence $D_{\parallel}^* / D_{\perp}^* \approx (\frac{c}{a})^2 \approx 0.42$ which is close to the measured value.

3.2 Impurity diffusion in TiO₂

Peterson and Sasaki [12, 13] have measured tracer diffusion of a selection of impurities both parallel and perpendicular to the c -axis. They discovered that both the rate and anisotropy of diffusion vary greatly with the impurity. For example, Zr diffuses slowly and D_{\parallel}^* is slightly less than D_{\perp}^* , as for Ti. On the other hand Co diffuses very rapidly and the anisotropy is very different D_{\parallel}^* being much greater (by about 10^3) than D_{\perp}^* . Some of the experimental data for Sc, Fe and Co are compared with D_{Ti}^* in Fig 2. The similar dependence of D^* on a_{O_2} for Sc, Ti and Fe (for $a_{O_2} < 10^{-5}$) shows that the Ti interstitial defect participates in the diffusion of the impurities.

This general behaviour may be understood qualitatively in the following way, if it is assumed that the lower the valency of the ion the more easily can it make direct interstitial jumps. Thus the tetravalent and trivalent ions (Zr^{4+} and Sc^{3+}) diffuse by an interstitialcy mechanism alone (like Ti itself). The divalent ions (Fe^{2+} and Co^{2+}), however, diffuse by a mixture of interstitialcy jumps and much faster direct interstitial jumps along the channels parallel to the c -axis. This process is illustrated schematically in Fig.3. The sudden decrease in D_{Co}^* and D_{Fe}^* as a_{O_2} rises above about 10^{-3} could perhaps be caused by the oxidation of these ions to the trivalent state [12].

4. NiO, CoO, MnO and FeO

These oxides all have the rocksalt crystal structure and are cation deficient; conventionally written $M_{1-x}O$. Cation vacancies, generated according to equation (1), are responsible for the deviation from stoichiometry which increases in the order NiO, CoO, MnO and FeO. There

has been a great deal of work carried out on the properties of these oxides and several reviews have appeared recently [14, 15, 16]. These will not be reiterated here, but some of the main conclusions regarding the most appropriate point defect parameters and the interactions between point defects will be examined.

4.1 Point defects and cation self diffusion

Peterson and Wiley [17] have recently compiled and analysed data for x , D_{Ni}^* and σ for NiO which they fitted to a model which allows V_{Ni}'' and V_{Ni}' together with compensating holes. The two types of defect are required because the exponent n is found to vary with a_{O_2} and T between the limits of 0.167 and 0.25 which would be expected if only V_{Ni}' or V_{Ni}'' need be considered. Similar defect models based on x and σ had been developed earlier by Koel and Gellings [18] and Farhi and Petot-Ervas [19]. The model of Koel and Gellings was also found to be consistent with D_{Ni}^* in pure and Al-doped NiO [20]. The defect parameters produced by these various models are summarised in Table 2. All the models have the common feature that singly charged vacancies are dominant, but doubly charged vacancies make a significant contribution at high T and low a_{O_2} . Despite this similarity the parameters for the different models show wide variation. This is particularly apparent for h_m in the two models of Peterson and Wiley, both of which give equally good fits to the experimental data. Peterson and Wiley eventually favour model A on the grounds that when combined with chemical diffusion data it gives a slightly more acceptable correlation factor for nickel self-diffusion than either model B or that of Koel and Gellings. However, this is probably not a reliable way of distinguishing between different models since it is based on the synthesis of different measurements on a range of specimens from different sources. It is probably more meaningful to compare the different models on the basis of their physical plausibility. First, consider the energy of association between the doubly charged vacancy and a hole to form a singly charged vacancy. Since the coulomb interaction between V_{Ni}'' and h_m is attractive the enthalpy change for the association reaction

$$\Delta h_f = h_f(V_{Ni}^{\cdot}) - h_f(V_{Ni}^{\cdot\cdot}) \quad (8)$$

is expected to be negative. All the models for NiO satisfy this criterion. Furthermore, atomistic calculations [21] suggest that in all these oxides $\Delta h_A = -0.5$ eV. The model of Peterson and Wiley gives $\Delta h_A = -1.87$ eV, which is an extremely strong interaction energy. The model of Koel and Gellings ($\Delta h_A = -1.08$ eV) is more acceptable from this point of view. Secondly, the large difference in h_m for the singly charged and doubly charged vacancies in Peterson and Wiley model A is unexpected since the hole has a much higher mobility than the vacancy and is unlikely to require complete dissociation from the vacancy to allow the vacancy to jump (which is what model A implies). On this basis it would seem that the model of Koel and Gellings (Table 2a) represents the best compromise between a fit to the experimental data and reasonable parameter values.

The results of atomistic calculations of the energies for creation and migration of cation vacancies in NiO are shown in Table 3 and may be compared with the corresponding enthalpies deduced from the experiments (Table 2). The level of agreement between theory and experiment can only be described as fair; the calculated formation energies (2.2 and 1.5 eV) being somewhat less than measured (2.8 eV) and the calculated migration energies (2.2 and 2.4 eV) being somewhat greater than measured (1.6 eV).

The deviation from stoichiometry in CoO is larger than in NiO, with $x \approx 10^{-2}$ at $a_{O_2} = 1$ [24]. Consequently interactions between defects are more important and there is general agreement that the singly charged vacancy is dominant but both V_{Co}^{\cdot} and $V_{Co}^{\cdot\cdot}$ make significant contributions under appropriate conditions. Dieckmann [25] has analysed data for ΔG_{Co}^* , x and σ in terms of such a defect model and the resulting parameters are given in Table 2. These parameters are physically acceptable in that the association enthalpies are small and negative (~ -0.3 eV) and the migration enthalpy is independent of the effective charge of the vacancy. The main question which is unresolved is whether more extensive associated defects are formed at large deviations from stoichiometry. Some evidence for this comes from electrical

conductivity measurements by Petot-Ervas et al [26]. They found that at $a_{O_2} \sim 1$, $n_V \sim 0.3$ (whereas the maximum allowed by Dieckmann's model is $n_V = 0.25$) and suggested that charged clusters of defects may be responsible for this behaviour.

Deviation from stoichiometry in MnO can reach greater levels than in CoO ($x \approx 10^{-1}$ at 1300°C). Recently Keller and Dieckmann [27] have measured x for MnO and analysed these results and Mn tracer diffusion measurements in terms of manganese vacancies with effective charges 2, 1 and 0. Their defect parameters are summarised in Table 2 (Model A). They indicate that doubly charged and neutral vacancies are dominant with only a small contribution from singly charged vacancies. The formation enthalpies of the dominant defects are negative reflecting the experimental observation that increasing T at constant a_{O_2} causes the deviation from stoichiometry to decrease. However, the relative magnitudes of h_f for the three vacancy types are difficult to accept; in particular it would seem that the interaction between $V_{Mn}^{''}$ and h is repulsive but attractive between V_{Mn}^{\cdot} and h . Keller and Dieckmann also offer an alternative fit to the data (model B) in which only $V_{Mn}^{''}$ and h are allowed, but the interactions between them are treated in the Debye-Hückel approximation. This is also unsatisfactory since the theory is only valid for lower defect concentrations and, in order to fit the data, a thermally activated dielectric constant was necessary. An alternative explanation [21, 28] is that larger defect clusters are dominant at high a_{O_2} . Tetot and Gerdanian [29] have compared the predictions of such a model with experimental data for x and find no evidence to support the idea of clusters (at least for $x \leq 1.5 \times 10^{-2}$). The defect parameters from their fit to the data are also shown in Fig 2. (The values tabulated are internal energies at 0K rather than h_f). Their tabulated figures have been adjusted to the appropriate defect formation reaction as indicated in Appendix 2 of their paper. These parameters are more plausible since h_f decreases as the charge on the vacancy decreases as expected. As pointed out by Keller and Dieckmann there is a direct proportionality between D_{Mn}^+ and x at a given temperature. This also argues against the formation of appreciable

quantities of clusters. In MnO at low a_{O_2} , where it is close to stoichiometry, it has been suggested that manganese interstitials are dominant. The experiments of Keller and Dieckmann are however not consistent with this hypothesis and they conclude that the stoichiometric composition, if it exists at all, must be very close to the Mn/MnO phase boundary. The n-type conduction in MnO at low a_{O_2} is then attributable to electrons having much greater mobility than holes.

In FeO there is no doubt that defect clusters exist since they have been identified by diffraction studies. Interaction between defects is so strong that D_{Fe}^* is not related in any simple way to x in this material [14]. Indeed, at 1000°C D_{Fe}^* is practically independent of x (for $0.05 < x < 0.13$). Thus although iron diffusion is believed to take place by vacancies not bound in clusters, there is no satisfactory model of diffusion and defects in FeO. The influence of the clusters on iron diffusion in FeO is apparent not only in the unexplained relationship between D_{Fe}^* and x , but also in the isotope effect for D_{Fe}^* . From such measurements Chen and Peterson [36] deduce that the correlation factor, f , for D_{Fe}^* is only about half that for diffusion in the fcc lattice by an isolated vacancy mechanism. They also find similarly low values of f for D_{Mn}^* in MnO [37]. Whilst this suggests that defect clusters may be formed in MnO, the very different relationship between D^* and x in the two oxides implies that the similarity in f may be fortuitous.

Calculations of h_m for cation vacancy migration in all these oxides have been carried out and are compared with experiment in Fig 4. The agreement is good for MnO (as it is for MgO which is also shown), but is poor for NiO and CoO.

4.2 Oxygen self diffusion

In recent years there have been several studies of oxygen self diffusion in these four oxides and Arrhenius plots of L_{xy}^* at constant a_{O_2} (except for FeO which is for constant CO_2/CO ratio) are presented in

Fig 5. The general trends in the magnitude of D_{oxy}^* and its activation energy are as would be expected from the relative melting temperatures of the oxides. The data of Yamaguchi and Someno [31] for CoO have an activation energy of 3.0 eV which is significantly lower than the 4.5 eV reported by Routbort and Rothman [32]. In view of the magnitude of D_{oxy}^* for CoO when compared to that for NiO and MnO (Fig 5) it seems reasonable to conclude that the higher activation energy is the correct one for CoO.

The point defects by which oxygen diffuses in these oxides have yet to be confidently identified. Measurements of D_{oxy}^* in CoO have been reported by Clauss et al [34] and are reproduced in Fig 6. The vee-shaped curve indicates that at high a_{O_2} oxygen interstitials are responsible for oxygen diffusion and at low a_{O_2} , vacancies. Clauss et al suggest that the most likely defects are uncharged interstitials and doubly charged vacancies.

Dubois et al [35] measured D_{oxy}^* in NiO at two values of a_{O_2} over a range of temperature. They found that decreasing a_{O_2} gave a lower D_{oxy}^* at the higher temperatures ($\sim 1500^\circ\text{C}$), but had little effect at lower temperature ($\sim 1300^\circ\text{C}$). They suggest that an uncharged interstitial could be the diffusing defect at high temperature and a doubly charged vacancy at low temperature. If this is the case the activation energy for D_{oxy}^* by the interstitial mechanism has to be greater than that for the vacancy mechanism.

Data for D_{oxy}^* in FeO as a function of a_{O_2} are shown in Fig 6. Again these suggest diffusion by an interstitial oxygen defect, but since the behaviour of the majority defects in FeO is still obscure it is dangerous to draw any conclusions at this stage.

Although oxygen interstitials are implicated in the experimental evidence, their presence is at first sight surprising for a large ion in a close-packed sublattice. Nevertheless, calculations of the formation

and migration energies of oxygen defects [4, 22, 23] tend to support their role in oxygen diffusion. The calculations suggest that D_{oxy}^* would have an activation energy of about 9 eV for a vacancy mechanism and 5 - 6 eV for an interstitialcy mechanism. This latter value is in good agreement with the experimental value of 5.6 eV [20], but the higher activation energy calculated for the vacancy mechanism is not consistent with the suggested interpretation of the oxygen activity dependence [35].

4.3 Behaviour of impurities

The behaviour of impurities in oxides is of interest both as dopants influencing self diffusion or as diffusing species themselves. Several studies of both types have been reported in the rocksalt oxides; particularly CoO and NiO.

The influence of an impurity on self diffusion depends on the site it adopts (substitutional or interstitial), its charge and how strongly it interacts with native point defects. It is not straightforward to be sure which charge state of a transition metal impurity will be the stable one in a transition metal oxide. Stoneham and Sangster [38] have studied this question from the theoretical viewpoint. By comparing ionisation energies of the bare ions they conclude that holes should be preferentially attracted from Ni to divalent Cr, Mn, Fe and Co ions in NiO, but only to Cr and Fe from Co in CoO. However, in both oxides none of these impurities is capable of reaching the 3+ charge state by creating a conduction band electron (e.g. Ni^+). The attraction between impurity and hole is such that dilute Cr and Fe impurities in CoO could be in 3+ charge state whereas Ni and Mn in CoO should be in the 2+ charge state. If stabilisation of the 3+ charge state is strong enough then impurity concentrations greater than the native hole concentration will tend to form charge-compensating cation vacancies and have a relatively large effect on self diffusion of the host cation. Experiments tend to support these ideas. For example, Co doping of NiO does not have much effect on Ni diffusion [39] which is consistent with Co^{2+} being predominant. In Al-doped NiO, Al^{3+} is stable which causes an appreciable increase in $[V_{\text{Ni}}^+]$ (and hence D_{Ni}^+ [20]) and chromium behaves

similarly indicating Cr^{3+} [40]. Measurements of D_{Co}^* and D_{Fe}^* in Fe-doped CoO [41], however, suggest that Fe is present as both Fe^{2+} and Fe^{3+} ; their ratio depending on a_{O_2} . Studies of diffusion in doped oxides enable an estimate to be made of the enthalpy of association, Δh_A , between the impurity and the point defects responsible for diffusion. Values of Δh_A deduced in this way for impurities associating with vacancies in NiO are - 1.2 eV for Al and - 0.6 eV for Cr [20]. Some calculated values for association are given in Table 3. For Al^{3+} the association energy is negative as expected for the coulombic attraction between defects having opposite effective charge, but is considerably smaller in magnitude than the experimental value.

The diffusion of impurity tracers themselves (at sufficiently low concentration not to influence the native point defect concentrations) can be extremely complicated. If the impurity diffuses by the same point defect (say a vacancy) as the host, the ratio of their tracer diffusion coefficients is given by [42]

$$\frac{D_2^*}{D_0^*} = \frac{w_2}{w_0} \frac{f_2}{f_0} \cdot \exp(-\Delta h_A/kT) \quad (9)$$

provided that $|\Delta h_A|$ is small enough. In this equation the subscript 2 denotes the impurity and w_2 is the jump frequency of an impurity/vacancy exchange. The correlation factor for the impurity, f_2 , is a complicated function of all the jump frequencies in the vicinity of the impurity. It is approximately bounded by $f_2(\text{min}) \approx \frac{w_0}{w_2}$ when $w_2 \gg w_0$ and $f_2(\text{max}) = 1$ when $w_2 \ll w_0$.

Tracer diffusion coefficients for a range of cation impurities in CoO and NiO have been reported by Hoshino and Peterson [43] and Monty [14]. In general, the results show a trend in which small ions diffuse more slowly than large ones and have larger activation energies for D_2^* . (There are exceptions, however, such as Ca^{2+} which is large and diffuses slowly). Theoretical estimates of the activation energy of w_2 (Table 3) do not reproduce this trend for divalent impurity ions. In particular,

particular, the measured activation energy of D_2^* for Fe and Mn in NiO is about 0.7 eV lower than of D_{Ni}^* , which is not expected from Table 3. Indeed, it is difficult to envisage such low activation energies for any divalent ions. This is because even if the impurity jump w_2 is very fast the limiting value of f_2 is approximately w_0/w_2 and hence D_2/D_0 is the limiting value $\exp(-\Delta h_A/kT)$. Physically, this corresponds to the impurity repeatedly exchanging with the same vacancy. A low activation energy can thus only occur if Δh_A is appreciable and negative (in this case about - 0.7 eV). This could be explained if Fe and Mn are present as trivalent ions in NiO, which would be consistent with theoretical predictions at low concentrations (by capture of a hole).

5. Fe₃₋₄O₄ (magnetite)

Magnetite at low temperature (below 575°C) has the inverse spinel structure. The structure is formed by the cubic close packing of oxygen ions as in the rocksalt structure. However, in the rocksalt structure the cations only occupy the octahedrally co-ordinated interstices between the oxygen ions whereas, in the spinel structure, they are distributed over both octahedral and tetrahedral sites. In magnetite Fe³⁺ ions occupy tetrahedral sites and the octahedral sites are occupied half by Fe³⁺ and half by Fe²⁺. Above the Curie temperature the charge distribution of the Fe ions becomes more random i.e. Fe²⁺ ions occupy some of the tetrahedral sites.

The properties of magnetite have been investigated extensively by Dieckmann and colleagues. Studies of deviation from stoichiometry (conventionally written Fe_{3-x}O₄) have revealed that at high a_{O_2} Fe vacancies are dominant and at low a_{O_2} interstitials are dominant [44]. The stoichiometric point is approximately midway in the stability field of Fe₃O₄. At the stoichiometric composition the disorder is of the cation Frenkel type, but is considerably more complicated because of the different cation sites and the charge state disorder. Dieckmann found that at the stoichiometric composition the defect concentration does not have simple Arrhenius behaviour but has an activation energy 0.9 eV for T below 1300°C and 2.5 eV for T above 1300°C. Lewis et al [45] have

calculated the energies to form defects in Fe_3O_4 and conclude that cation vacancies and interstitials are preferentially on the octahedral sites. From their calculations they deduce that the activation energy for Frenkel disorder is 3 eV. This is much greater than the 0.9 eV observed at low temperature (where the best agreement would be expected). Furthermore, the calculations cannot account for the non Arrhenius behaviour (which experiment shows has its origin in the interstitial contribution).

The tracer self diffusion of iron in magnetite as a function of a_{O_2} reflects the expected contributions of vacancies and interstitials at high and low a_{O_2} respectively [46]. Both Co and Cr tracer diffusion coefficients [47] show a similar dependence on a_{O_2} to D_{Fe}^* which indicates that Co and Cr (and therefore probably Fe) diffuse by an interstitialcy mechanism at low a_{O_2} . This is supported by measurements of isotope effect for D_{Fe}^* as a function of a_{O_2} [48]. Dieckmann [24] has also reported values for the diffusion coefficients of the vacancies and interstitials derived both from chemical diffusion and D_{Fe}^* and x . His results are reproduced in Fig 7 which clearly illustrate that both the interstitial and vacancy have non-Arrhenius behaviour. At the lowest temperatures the migration enthalpies are about 0.7 eV for the vacancy and 2.0 eV for the interstitial. The corresponding estimates of Lewis et al [45] are 1.60 eV for the vacancy and 0.92 for the interstitial neither of which are in good agreement with experiment.

6. Fe_2O_3 (hematite) and Cr_2O_3 (chromite)

Both these oxides have the corundum structure in which the oxygen ions are arranged in almost hexagonal close packing with the trivalent metal ions situated in two thirds of the octahedrally co-ordinated interstices. In both oxides the nature of the dominant point defects is not yet clearly established.

6.1 Fe_2O_3

There is general agreement that Fe_2O_3 is oxygen deficient ($\text{Fe}_2\text{O}_{3-x}$).

and that the dominant defects must be either oxygen vacancies or iron interstitials. There is also general agreement that at high temperatures Fe_2O_3 is an intrinsic electronic semiconductor with a thermal band gap of about 2eV. This is based on the observation that the electrical conductivity is independent of a_{O_2} [49] and there is strong optical absorption at 2.1 eV [50].

Recent measurements of D_{Fe}^* parallel to the c direction at $a_{\text{O}_2} = 1$ are summarized in Fig 8. The results are in reasonably good agreement at high temperatures and the activation energy is 6.0 eV. Nevertheless, the difference between the two sets of results from Hoshino and Peterson [52, 53] are significant since they were performed on crystals from different sources. Chang and Wagner [49] and Hoshino and Peterson [52, 53] measured D_{Fe}^* as a function of a_{O_2} . All agree that the exponent n_D is negative indicating that iron interstitials are responsible for diffusion. However, the value of n_D is not well established. Chang and Wagner found $n_D = -0.7$ and Hoshino and Peterson [53] measured the same value for crystals from the same source, but the actual magnitudes of D_{Fe}^* were about ten times greater. Crystals from a different source [52] gave lower values of D_{Fe}^* and $n_D = -0.4$. The simplest model involving Fe^{3+} interstitial ions predicts $n_D = -0.75$, in good agreement with the first set of experiments. In the same crystals Hoshino and Peterson found $D_{\text{Co}}^* > D_{\text{Fe}}^* > D_{\text{Cr}}^* > D_{\text{Y}}^*$, but all had similar values of n_D . As in Fe_3O_4 , this indicates that they all diffuse by an interstitialcy mechanism rather than direct interstitial jumps and this is again supported by the isotope effect measurements [52].

The break in the Arrhenius plot of D_{Fe}^* at about 900°C observed by Atkinson and Taylor [51] (Fig 8) is also seen in measurements of electrical conductivity. The most likely explanation of this behaviour is that below 900°C these crystals are extrinsic p-type semiconductors with divalent cation impurities as acceptors.

In conclusion, although there are some inconsistencies in the experimental data, the most likely defect picture is that at high temperatures and oxygen pressures Fe_2O_3 is an intrinsic semiconductor with oxygen vacancies as majority ionic defects and iron interstitials as minority ionic defects. Iron diffuses by an interstitialcy mechanism. At low temperatures behaviour is dominated by divalent cation impurities compensated by electron holes.

6.2 Cr_2O_3

In contrast with Fe_2O_3 , Cr_2O_3 appears to be cation deficient at $a_{\text{O}_2} = 1$ (i.e. $\text{Cr}_{2-x}\text{O}_3$) with chromium vacancies being the dominant ionic defects. The strongest evidence for this comes from measurements of x in Cr_2O_3 (as coarse powder) as a function of a_{O_2} at 1100°C by Greskovich [54]. He found that x (typically about 10^{-4} at this temperature) increases with increasing a_{O_2} with an exponent $n_x = 0.12$. If $V_{\text{Cr}}^{3'}$, compensated by electron holes, is responsible for deviation from stoichiometry then n_x would be expected to be 0.188 as also would n_σ and n_D (for D_{Cr}^*). (If U_{Cr}^{2+} is the dominant defect then $n_x = n_\sigma = 0.167$ and $n_D = 0.50$).

Studies of electronic conductivity on sintered material however, do not support this simple view. Matsui and Naito [55] report that n_σ (at high a_{O_2}) decreases with increasing temperature; being 0.08 at 1000°C and 0.05 at 1100°C . Similar experiments by Nagai et al [56] confirmed this effect, with n decreasing from 0.13 at 600°C to 0.04 at 1200°C . These observations suggest at first sight that Cr_2O_3 is tending towards being an intrinsic semiconductor at the higher temperature. Furthermore, Matsui and Naito also observed a change of sign in n_σ at low a_{O_2} which indicates that n-type behaviour is dominant under these conditions. This could be explained by a variety of different mechanisms e.g. higher mobility of electrons than holes (as in MnO), a change in point defects from say $V_{\text{Cr}}^{3'}$ to $\text{Cr}_i^{3\cdot}$, or a change in valency of an impurity.

The change from p-type conduction at high a_{O_2} to n-type at low a_{O_2} was confirmed by thermoelectric power measurements on sintered Cr_2O_3 by Young et al [57, 58]. They also revealed an important experimental difficulty which may account for some of the apparently irreconcilable observations which have been made on this material. They found that conversion between n and p-type material was not equally facile in both directions. In particular, the p to n transition is severely hindered kinetically at temperatures below 1500°C (Fig 9). They also argue that the magnitude of the thermoelectric power and the activation energy of σ at high temperature in the p-type region (1.8 eV) can only be explained if the thermal band gap in Cr_2O_3 is larger than 3.6 eV.

There have also been several studies of electrical conductivity in doped sintered Cr_2O_3 . For example Huang et al [59] studied Li-doped Cr_2O_3 at temperatures between 815 and 1100°C. They found that σ was independent of a_{O_2} ($n_\sigma = 0$) at high a_{O_2} and $n_\sigma = 0.25$ at low a_{O_2} . This is consistent with p type behaviour in the doped material and a p to n transition in undoped Cr_2O_3 . (At low a_{O_2} , n_σ in Li doped Cr_2O_3 is expected to be 0.25 if either Cr_1^{3+} or V_O^{2+} is dominant in pure Cr_2O_3 . Therefore these experiments cannot be used to differentiate between the two possible defects).

Studies of D_{Cr}^* in Cr_2O_3 are not easily interpreted bearing in mind this rather confused picture of electrical properties. The most recent data are shown in Fig 10. These diffusion coefficients are very much lower than those reported earlier (see ref 3). They are believed to be more reliable than earlier measurements because of improved techniques and materials and because at 1100°C they are in good agreement with D^* estimated from x and chemical diffusion [54]. At high a_{O_2} at both 1570°C and 1100°C the dependence of D_{Cr}^* on a_{O_2} is close to that expected for diffusion by V_{Cr}^{3+} . For low a_{O_2} at 1100°C and 1300°C there is an indication of diffusion by chromium interstitials, but the evidence is not strong. In fact the rather strange behaviour at high a_{O_2} and 1300°C

in Fig 10 strongly suggests that equilibration between the gas and the solid is unreliable.

At the present time it seems that Cr_2O_3 is not an intrinsic semiconductor as originally supposed, but has a band gap of at least 3.6 eV. It is p-type at high a_{O_2} due to the formation of chromium vacancies (and holes) and n-type at low a_{O_2} due to chromium interstitials (and electrons). There are severe experimental problems in this system the most serious of which is the unreliable equilibration with the gas phase. The activation energy for Cr diffusion in the p-type region at constant a_{O_2} is about 6.0 eV [61].

7. Cu_2O (cuprite)

Cuprous oxide is a copper deficient p-type semiconductor (Cu_{2-x}O) with defect properties very similar to those of the rocksalt oxides, although it has a very different crystal structure. Experimental data are available for x , σ , D_{Cu}^* and D_{oxy}^* . Simple defect models predict n_x and n_{D} (for Cu) should be 0.125 for singly charged copper vacancies and 0.25 for neutral vacancies (and $n_{\sigma} = 0.125$). In common with the other oxides the experimental values fall between the two extremes with n depending on both a_{O_2} and T . Data for D_{Cu}^* and 1000°C are shown in Fig 11 [62] and indicate that V_{Cu}' is the dominant defect with a contribution from V_{Cu}^x at high a_{O_2} . Peterson and Wiley [62] have fitted all the data to a defect model involving the two copper vacancies and singly charged oxygen interstitials. The oxygen interstitials are invoked to account for the observation that $n_{\sigma} > 0.125$ at high a_{O_2} and are consistent with the effect of a_{O_2} on D_{oxy}^* observed by Perinet et al [63] and also shown in Fig 11. The point defect parameters from Peterson and Wiley's fit to the experimental data are summarised in Table 4. Equal enthalpies of motion for the two charge states of the vacancy are expected (as discussed earlier for the other oxides) but equal enthalpies of formation are not, since this means the binding energy between the vacancy and the hole is negligible. According to Table 4 the binding between the vacancy and the hole is entirely due to

entropy changes. Thus although these parameters describe the experimental data, their validity is questionable. Ochin et al [64] have suggested that the formation of divacancies ($V_{Cu}^{\cdot} V_{Cu}^{\times}$)' at high a_{O_2} and copper interstitials at low a_{O_2} can account for their electrical conductivity data. However, the measurements of D_{Cu}^* show no indication of a substantial contribution from copper interstitials and there is no other evidence to support the existence of divacancies.

8. Diffusion along grain boundaries and dislocations

The subject of fast diffusion along grain boundaries and dislocations has been reviewed in recent articles by Atkinson [65, 66] and Atkinson and Le Claire [67]. The most comprehensive data are for NiO and these are summarised in Fig 12 compared with diffusion in the bulk lattice. The diffusion of both Ni and O are greatly enhanced in grain boundaries and dislocations compared with corresponding lattice diffusion. The width of the region of enhanced diffusivity has been shown [68, 69] to be only about 10 Å and both dislocation and grain boundary diffusion of Ni in NiO depend on a_{O_2} in a similar way to lattice diffusion. This suggests that grain boundary and dislocation diffusion take place by a similar mechanism to lattice diffusion; in this case by nickel vacancies which segregate to the extended defects from the lattice. This similarity is reinforced by studies of impurity diffusion in NiO grain boundaries [71] for which similar trends to lattice diffusion have been found. Atomistic simulations of the structure and diffusive properties of dislocations [72] and grain boundaries [22] support this view. Duffy and Tasker [22] have made a detailed theoretical study of grain boundaries and their properties in NiO [22]. Their calculations for a range of boundary misorientations predict that the activation energy for D_{Ni}^* in the boundary should be between 0.5 and 0.8 of that in the lattice. The experimental value of this ratio in polycrystalline material (and therefore covering a range of boundary types) is 0.70. The corresponding ratio for oxygen diffusion (assuming an interstitialcy mechanism) is 0.45 from both calculations and experiment. The agreement between theory and experiment on this basis is therefore very encouraging (although the

absolute values of activation energies and defect parameters are not in such good accord; see section 4.1).

9. Concluding remarks

Perhaps the most striking general feature to emerge from considering this group of oxides is that simple defect models (i.e. with a single pair of charge-compensating defects for each oxide) are not appropriate other than as a first order approximation. The approach that most workers have taken to solve this problem has been to allow more defect types in the model; particularly those in which the prime defect traps an electronic carrier. It appears that this is not necessarily a fruitful route to follow too far for two reasons. The first is that the deviation from the simple models, although significant, are often quite small and are apparent mainly at extremes of the experimental conditions (e.g. high T and low a_{O_2}). The fitting of more complicated models to the experimental data is therefore unreliable and, as we have seen, often leads to parameters describing the defects which appear physically unreasonable. The second problem in this approach is that the defect models still rely on the use of concentrations rather than thermodynamic activities in the mass-action equations. In this approximation strong short-range interactions between defects (such as the trapping of a hole at a vacancy) can be included by introducing an associated defect, but longer range screening interactions are ignored. At low defect concentrations these long range interactions can be described by the Debye-Hückel theory and although the effects are small they are nevertheless significant. For example Wagner [73] estimates that when $x = 10^{-3}$ in $Cu_{2-x}O$ at $1000^\circ C$ the activity coefficient of each defect (V'_{Cu} or h) is reduced from unity (ideal non-interacting solution) to about 0.5. However, the introduction of screening interactions in the Debye-Hückel approximation cannot of itself account for all the observed deviations from simple defect models in these oxides as is evident, for example, from such an attempt applied to MnO [27]. In oxides with relatively large defect concentrations ($\geq 10^{-2}$) the Debye-Hückel approximation (i.e. regarding the defects as being distributed in a dielectric continuum) is no longer justifiable. For such cases theoretical treatments have been

developed [74], but are not convenient for analysing experimental data. Nevertheless, until some attempt is made to include deviations from ideality, the more complicated defect models, and some of their derived parameters, should not be taken too seriously.

Another general feature which emerges is the rather poor level of agreement between point defect parameters derived from experiment and those from calculations. Even bearing in mind the problems already referred to associated with assuming ideal thermodynamic activities for the defects, the level of agreement between experiment and theory is nowhere near as good as found in the alkali halides. This is particularly evident in h_m for vacancy - cation jumps and binding energies in the rocksalt oxides (Fig 4 and Table 3). It would appear that there are still significant processes specific to the transition metal oxides which the calculations are not yet taking into account. (The most recent calculations of Harding and Tarento reported in this volume have already resolved some of the discrepancies.) Nevertheless, the calculations are invaluable even at a semi-quantitative level since they point to trends, or rule out defect processes with highly unfavourable energy barriers.

On the experimental side, the quality of data and level of understanding for diffusion and defects on the cation sublattice is far superior to that of the anion sublattice. This is because the anion defects can only be studied by diffusion and these experiments are very difficult. Nevertheless, interest is building in this area and the situation is likely to improve considerably. Even the cation defects are not established and understood in the important oxides Fe_2O_3 and Cr_2O_3 . The question of larger defect clusters in oxides other than FeO is still open. The indirect evidence for their existence is appreciable only in MnO and direct observations are necessary to settle this question.

Finally, in the case of impurity diffusion it is interesting to note that the order of their diffusivities is almost independent of the matrix through which they are diffusing. For example, Mn is always a fast diffuser and Cr always a slow diffuser.

Acknowledgement

The author wishes to thank Dr J Harding and Dr P W Tasker for useful discussions.

REFERENCES

1. A.B. Lidiard, "Ionic conductivity", *Handbuch der Physik*, 20, 246-349 (1957).
2. F.A. Kröger, "The chemistry of imperfect crystals", North Holland, Amsterdam (1964).
3. P. Kofstad, "Nonstoichiometry, diffusion and electrical conductivity in binary metal oxides", John Wiley, New York (1972).
4. W.C. Mackrodt, "Defect energetics and their relation to nonstoichiometry in oxides", *Solid State Ionics*, 12, 175-188 (1984).
5. M.J.L. Sangster and A.M. Stoneham, "Calculation of absolute diffusion rates in oxides", *J. Phys. C: Solid State Phys.*, 17, 6093-6104 (1984).
6. K. Hoshino, N.L. Peterson and C.L. Wiley, "Diffusion and point defects in TiO_{2-x} ", *J. Phys. Chem. Solids*, 46[12], 1397-1411 (1985).
7. G.M. Raynaud and F. Morin, "Modelling of complex point defects in transition metal compounds", *J. Phys. Chem. Solids*, 46[12], 1371-1382 (1985).
8. N. Ait-Younes, F. Millot and P. Gerdanian, "Isothermal Transport in TiO_{2-x} - Part I, Electromigration in TiO_{2-x} ", *Solid State Ionics*, 12, 431-436 (1984).
9. Idem., "Isothermal Transport in TiO_{2-x} - Part II, Chemical diffusion in TiO_{2-x} ", *Solid State Ionics*, 12, 437-442 (1984).
10. R.N. Blumenthal, J. Coburn, J. Baukus and W.M. Hirthe, "Electrical conductivity of nonstoichiometric rutile single crystals from 1000 to 1500°C", *J. Phys. Chem. Solids*, 27, 643-654 (1966).
11. D.J. Derry, D.G. Lees and J.M. Calvert, "A study of oxygen self-diffusion in the c-direction of rutile using a nuclear technique", *J. Phys. Chem. Solids*, 42, 57-64 (1981).
12. J. Sasaki, N.L. Peterson and L.C. De Jonghe, "Fast diffusion of iron in single crystal rutile and iron-doped rutile", *Mat. Res. Soc. Symp. Proc.*, 24, 39-45 (1984).
13. N.L. Peterson and J. Sasaki, "Mechanisms of impurity diffusion in rutile", in 'Transport in Nonstoichiometric Compounds', Editors G. Simkovich and V.S. Stubican, Plenum, New York, (1985), 269-284.
14. C. Monty, "Diffusion in stoichiometric and non-stoichiometric cubic oxides", *Radiation Effects*, 74, 29-55 (1983).
15. N.L. Peterson, "Point defects and diffusion mechanisms in monoxides of iron-group metals", *Diffusion and Defect Data*, 36, 1-26 (1984).

16. N.L. Peterson, "Point defects and diffusion mechanisms in monoxides of iron-group metals", *Materials Science Forum*, 1, 85-108 (1984).
17. N.L. Peterson and C.L. Wiley, "Point defects and diffusion in NiO", *J. Phys. Chem. Solids*, 46(1), 43-52 (1985).
18. G.J. Koel and P.J. Gellings, "The contribution of different types of point defects to diffusion in CoO and NiO during oxidation of the metals", *Oxidation of Metals*, 5, 185-203 (1972).
19. R. Farhi and G. Patot-Ervas, "Electrical conductivity and chemical diffusion coefficient measurements in single crystalline nickel oxide at high temperatures", *J. Phys. Chem. Solids*, 39, 1169-1173 (1978).
20. A. Atkinson, A.E. Hughes and A. Hammou, "The self-diffusion of Ni in undoped and Al-doped NiO single crystals", *Philos Mag. A*, 43(5), 1071-1091 (1981).
21. C.R.A. Catlow and A.M. Stoneham, "Defect equilibria in transition metal oxides", *J. Amer. Ceram. Soc.*, 64(4), 234-236 (1981).
22. D.M. Duffy and P.W. Tasker, "Theoretical studies of diffusion processes down coincident tilt boundaries in NiO", Harwell Report TP1155, Harwell, Oxon, UK (1986).
23. M.J.L. Sangster and D.K. Rowell, "Calculation of defect energies and volumes in some oxides", *Philos. Mag. A*, 44(3), 613-624 (1981).
24. R. Dieckmann, "Point defects and transport properties of binary and ternary oxides", *Solid State Ionics* 12, 1-22 (1984).
25. R. Dieckmann, "Cobaltous oxide point defect structure and non-stoichiometry, electrical conductivity, cobalt tracer diffusion" *Z. Phys. Chem. N.F.* 107, 189-210 (1977).
26. G. Patot-Ervas, P. Ochin and B. Sossa, "Transport properties in pure and lithium doped cobaltous oxide", *Solid State Ionics* 12, 277-293 (1984).
27. M. Keller and R. Dieckmann, "Defect structure and transport properties of manganese oxides: (I) The nonstoichiometry of manganosite ($Mn_{1-x}O$)" *Ber. Bunsenges. Phys. Chem.* 89, 883-893 (1985).
28. A.M. Stoneham, S.M. Tomlinson, C.R.A. Catlow and J.H. Harding, "Clustering of defects: disorder of non-stoichiometric oxides", in 'Physics of disordered materials' Editors D. Adler, H. Fritzsche and S.R. Ovshinsky, Plenum, New York (1985) 243-252.
29. R. Tetot and P. Geranian, "Theoretical considerations regarding the defect structure of $M_{1-x}O$ cubic oxides for small departures from stoichiometry", *J. Phys. Chem. Solids* 46 (7) 869-879 (1985)
30. C. Dubois, C. Monty, and J. Philibert, "Oxygen self diffusion in NiO single crystals" *Philos. Mag. A* 46 (3) 419-433 (1982)

31. S. Yamaguchi and M. Someno, "The tracer diffusivity of oxygen in wustite and cobaltous oxide", *Trans. Jap. Inst. Metals* 23 (5) 259-266 (1982).
32. J.L. Routbort and S.J. Rothman, "Diffusion of ^{18}O in CoO in air" to be published in *J. Phys. Chem. Solids* (1986).
33. J.L. Routbort and K C Goretta, "Deformation and oxygen diffusion in $\text{Mn}_{1-\delta}\text{O}$ ", this volume.
34. C. Clauss, R.J. Tarento, C. Monty, A. Dominguez-Rodriguez, J. Castaing and J. Philibert, "Self diffusion and creep studies of the oxygen sublattice point defects in CoO " in 'Transport in Nonstoichiometric Compounds', Editors: G. Simkovich and V.S. Stubican, Plenum, New York, 255-268 (1985).
35. C. Dubois, C. Monty and J. Philibert, "Influence of oxygen pressure on oxygen self diffusion in NiO ", *Solid State Ionics* 12, 75-78 (1984).
36. W.K. Chen and N.L. Peterson, "Effect of the deviation from stoichiometry on cation self-diffusion and isotope effect in wustite, Fe_{1-x}O ", *J. Phys. Chem. Solids* 36, 1097-1103 (1975).
37. N.L. Peterson and W.K. Chen, "Cation self-diffusion and the isotope effect in $\text{Mn}_{1-\delta}\text{O}$ ", *J. Phys. Chem. Solids* 43 (1), 29-35 (1982).
38. A.M. Stoneham and M.J.L. Sangster "The diffusion of ions with multiple valence, the oxidation of transition metal alloys", *Philos Mag B* 52 (3) 717-727 (1985).
39. W.K. Chen and N.L. Peterson, "Cation diffusion semiconductivity and non-stoichiometry in $(\text{Co,Ni})\text{O}$ crystals", *J. Phys. Chem. Solids*, 34, 1093-1108 (1973).
40. N. Tabet, C. Dolin and C. Monty, "Hétérodiffusion d'éléments homovalents dans NiO pur et NiO dopé par Cr_2O_3 " *Rev Int. hautes Tempér, Refract., Fr.*, 19 413-416 (1982).
41. K. Hoshino and N.L. Peterson, "Diffusion and correlation effects in iron-doped CoO ", *J. Phys. Chem. Solids* 46 (2) 229-240 (1985).
42. A.D. Le Claire, "Diffusion", in 'Treatise on solid state chemistry Vol 4', Editor N.B. Hannay, Plenum, New York, 1-59 (1976).
43. K. Hoshino and N.L. Peterson, "Cation impurity diffusion in CoO and NiO ", *J. Phys. Chem. Solids* 45, 963-972 (1984).
44. R. Dieckmann, "Defects and cation diffusion in magnetite (IV): nonstoichiometry and point defect structure of magnetite ($\text{Fe}_{3-\delta}\text{O}_4$)" *Ber. Bunsenges. Phys. Chem.* 86 112-118 (1982).
45. G.V. Lewis, C.R.A. Catlow and A.N. Cormack, "Defect structure and migration in Fe_3O_4 ", *J. Phys. Chem. Solids* 46 (11) 1227-1233 (1985).

46. R. Dieckmann and H. Schmalzried, "Defects and cation diffusion in magnetite (I)", *Ber. Bunsenges. Phys. Chem.* 81, 344-347 (1977).
47. R. Dieckmann, T.O. Mason, J.D. Nodge and H. Schmalzried, "Defects and cation diffusion in magnetite III. Tracer diffusion of foreign tracer cations as a function of temperature and oxygen potential", *Ber. Bunsenges. Phys. Chem.* 82 778-783 (1978).
48. N.L. Peterson, W.K. Chen and D. Wolf, "Correlation and isotope effects for cation diffusion in magnetite", *J. Phys. Chem. Solids* 41 709-719 (1980).
49. R.N. Chang and J.B. Wagner, "Direct-current conductivity and iron tracer diffusion in hematite at high temperatures", *J. Amer. Ceram. Soc.* 55, 211-213 (1972).
50. D. Benjelloun, J.r. Bonnet and M. Onillon, "Anisotropy of electrical properties in pure and doped α -Fe₂O₃" in 'Transport in nonstoichiometric compounds', Editors G. Simkovich and V.S. Stubican, Plenum, New York, 51-60 (1985).
51. A. Atkinson and E.I. Taylor, "Diffusion of ⁵⁵Fe in Fe₂O₃ single crystals", *J. Phys. Chem. Solids* 46 (4), 469-475 (1985).
52. K. Hoshino and N.L. Peterson, "Cation self-diffusion and the isotope effect in Fe₂O₃" *J. Phys. Chem. Solids* 46 (3) 375-382 (1985).
53. K. Hoshino and N.L. Peterson, "Cation self-diffusion and impurity diffusion in Fe₂O₃", *J. Phys. Chem. Solids* 46 (11) 1247-1254 (1985).
54. C. Greskovich, "Deviation from stoichiometry in Cr₂O₃ at high oxygen partial pressures", *J. Amer. Ceram. Soc.* C-111-112 (1984).
55. T. Matsui and K. Naito, "Electrical conductivity anomaly of nonstoichiometric chromium sesquioxide", *J. Nucl. Mater.* 120 115-118 (1984).
56. H. Nagai, S. Ishikawa and K. Shoji, "Electrical conductivity of sintered Cr₂O₃ with Fe₂O₃", *Trans. Jap. Inst. Metals* 26 (1) 44-51 (1985).
57. E.W.A. Young, P.C.H. Stiphout and J.H.W. de Wit "n-type behaviour of chromium III oxide", *J. Electrochem. Soc.* 132 (4) 884-886 (1985).
58. E.W.A. Young, J.H. Gerretsen and J.H.W. de Wit, "The defect structure of chromium III oxide as a function of the oxygen partial pressure", in E.W.A. Young, Thesis, University of Utrecht, 76-84 (1986).
59. R.F. Huang, A.K. Agarwal and H.U. Anderson, "Oxygen activity dependence of the electrical conductivity of Li-doped Cr₂O₃", *Amer. Ceram. Soc.* 67 (2) 146-150 (1984).

60. K. Hoshino and N.L. Peterson, "Cation self diffusion in Cr_2O_3 ", J. Amer. Ceram Soc. 66 C-202-203 (1983).
61. A. Atkinson and R.I. Taylor, "Diffusion of ^{51}Cr in Cr_2O_3 and the growth of Cr_2O_3 films" in 'Transport in nonstoichiometric compounds' Editors G. Simkovich and V.S. Stubican, Plenum, New York, 285-295 (1985).
62. N.L. Peterson and C.L. Wiley, "Diffusion and point defects in Cu_2O " J. Phys. Chem. Solids 45 (C) 281-294 (1984).
63. F. Perinet, S. Barbesat and C. Monty, "New investigation of oxygen self diffusion in Cu_2O ", J. Phys. Paris Colloque C6 41 (7) 315-318 (1980).
64. P. Ochin, C. Petot and G. Petot-Ervas, "Thermodynamic study of point defects in Cu_{2-x}O . Electrical conductivity measurements at low oxygen partial pressures", Solid State Ionics 12, 135-143 (1984).
65. A. Atkinson, "Diffusion along grain boundaries and dislocations in oxides, alkali halides and carbides", Solid State Ionics 12, 309-320 (1984).
66. A. Atkinson, "Grain boundary diffusion - structural and mechanisms", J. Phys. Paris Colloque C4 46 (4) 379-5).
67. A. Atkinson and A.D. Le Claire, "What's new about pipe diffusion", in 'Dislocations 1984', Editors: P. Veysière, L. Kubin and J. Castaing, Editions du CNRS, Paris, 253-266 (1984).
68. A. Atkinson and R.I. Taylor, "The diffusion of Ni in the bulk and along dislocations in NiO single crystals", Philos. Mag. A 39, 581-595 (1979).
69. A. Atkinson and R.I. Taylor, "The diffusion of ^{63}Ni along grain boundaries in nickel oxide", Philos. Mag. A 43, 979-998 (1981).
70. A. Atkinson, F.C.W. Pummery and C. Monty, "Diffusion of ^{18}O tracer in NiO grain boundaries" in 'Transport in Nonstoichiometric Compounds', Editors G. Simkovich and V.S. Stubican, Plenum, New York, 359-370 (1985).
71. A. Atkinson and R.I. Taylor, "Impurity diffusion in NiO grain boundaries", J. Phys. Chem. Solids 47 (3) 315-323 (1986).
72. J. Rabier and M.P. Puls, "Atomistic model calculations of pipe diffusion mechanisms in MgO ", Philos. Mag. A, 52 (4) 461-477 (1985).
73. C. Wagner, "Equations for transport in solid oxides and sulphides of transition metals", Prog. Solid State Chem. 10, 216-277 (1977).
74. A.R. Alnatt and E. Loftus, "Physical cluster theory of point defect interactions I. General formalism II Application to F_2 in CaF_2 and CdCl_2 ", J. Chem. Phys., 59 2541-2559 (1973).

Table 1
Defect parameters for TiO₂

<u>Formation reaction</u>	<u>Δ_f/k</u>	<u>$\frac{h_f}{(eV)}$</u>	<u>$\frac{h_m}{(eV)}$</u>
$TiO_2 \rightarrow Ti_1^{4\cdot} + 4e' + O_2$	37.9	10.67	0.68
$TiO_2 \rightarrow Ti_1^{3\cdot} + 3e' + O_2$	24.9	9.24	0.68
$\frac{1}{2}TiO_2 \rightarrow V_O^{\cdot\cdot} + 2e' + \frac{1}{2}O_2$	-	-	2.9

Table 2

Experimental defect parameters for NiO, CoO and MnO

<u>Source</u>	<u>Defect*</u>	<u>s_f/k</u>	<u>h_f</u>	<u>h_m</u>
(a) NiO				
Peterson and Wiley model A [17]	V_{Ni}''	1.6	3.69	0.59
	V_{Ni}'	-2.3	1.82	2.10
Peterson and Wiley model B [17]	V_{Ni}''	1.6	3.69	1.32
	V_{Ni}'	-2.3	1.82	1.60
Koel and Gellings [18] + Atkinson et al. [20]	V_{Ni}''	-5.0	2.81	1.60
	V_{Ni}'	-3.2	1.73	1.60
Farhi and Petot-Ervas [19]	V_{Ni}''	-	2.9	-
	V_{Ni}'	-	1.5	-
(b) CoO				
Dieckmann [25]	V_{Co}''	-5.0	1.55	1.41
	V_{Co}'	-3.2	0.80	1.41
	V_{Co}^x	-4.1	0.27	1.41
Petot-Ervas et al. [26]	V_{Co}'	-2.1	0.78	-
(c) MnO				
Keller and Dieckmann Model A [24]	V_{Mn}''	-15.1	-0.94	1.73
	V_{Mn}'	-3.7	0.14	1.73
	V_{Mn}^x	-5.0	-0.81	1.73
Ide, Model B	V_{Mn}''	-13.5	-0.86	1.73
Tetot and Gerdanian [29]	V_{Mn}''	-6.4	2.1	-
	V_{Mn}'	1.8	-0.14	-
	V_{Mn}^x	-15.0	-1.15	-

* The formation reaction for a defect is $\frac{1}{2} O_2 + V_{Ni}^x + Ni^{2+} \rightarrow NiO$

Table 3

Calculated point defect energies (eV) for NiO

(a) Ni vacancies in NiO

$\frac{1}{2} O_2 \rightarrow V_{Ni}'' + 2 h' + O_O^x$	2.2 (ref. 4), 1.5 (ref. 22)
$V_{Ni}'' + h' \rightarrow V_{Ni}'$	-0.53 (ref. 21)
$V_{Ni}'' \rightarrow Ni_{Ni}^x$ jump	2.2 (ref. 4), 2.4 (ref. 22), 2.4 (ref. 23)

(b) Impurities in NiO (ref. 4)

<u>Impurity</u>	<u>Impurity + vacancy → associated pair</u>	<u>Impurity/vacancy jump</u>
Mg ²⁺	-0.07	2.43
Ca ²⁺	-0.25	2.35
Mn ²⁺	-0.12	2.43
Fe ²⁺	0.04	2.31
Co ²⁺	0.06	2.28
Al ³⁺	-0.41 (-1.2 expt)	3.53

Table 4

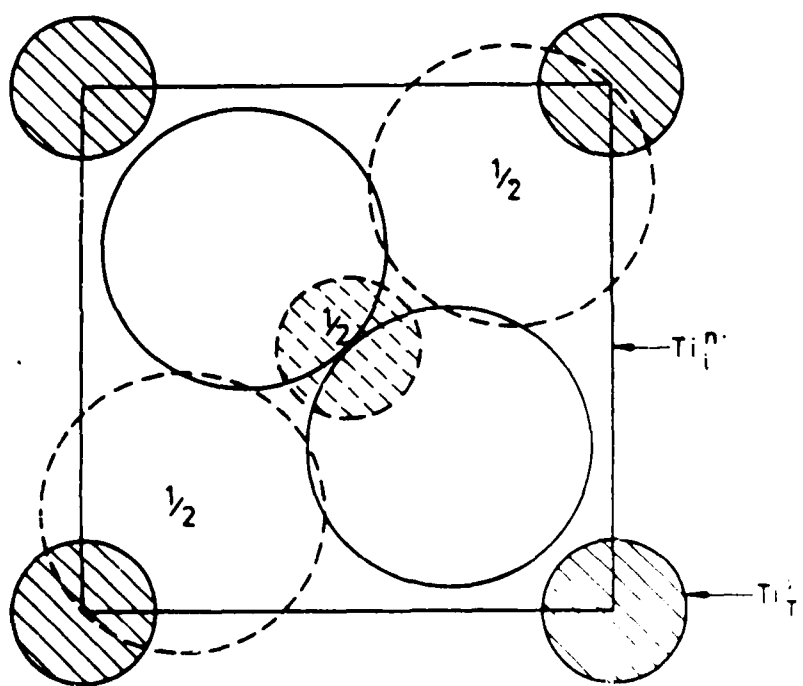
Point defect parameters for Cu₂O [62]

<u>Formation reaction</u>	<u>$\frac{e_f}{k}$</u>	<u>$\frac{h_f}{(eV)}$</u>	<u>$\frac{h_a}{(eV)}$</u>
$\frac{1}{2} O_2 \rightarrow V_{Cu}' + h + \frac{1}{2} O_O^x$	-2.5	1.28	0.42
$\frac{1}{2} O_2 \rightarrow V_{Cu}^x + \frac{1}{2} O_O^x$	5.4	1.28	0.42
$\frac{1}{2} O_2 \rightarrow O_i' + h$	-1.66	1.37	0.84

TiO₂ (rutile)

c-axis projection

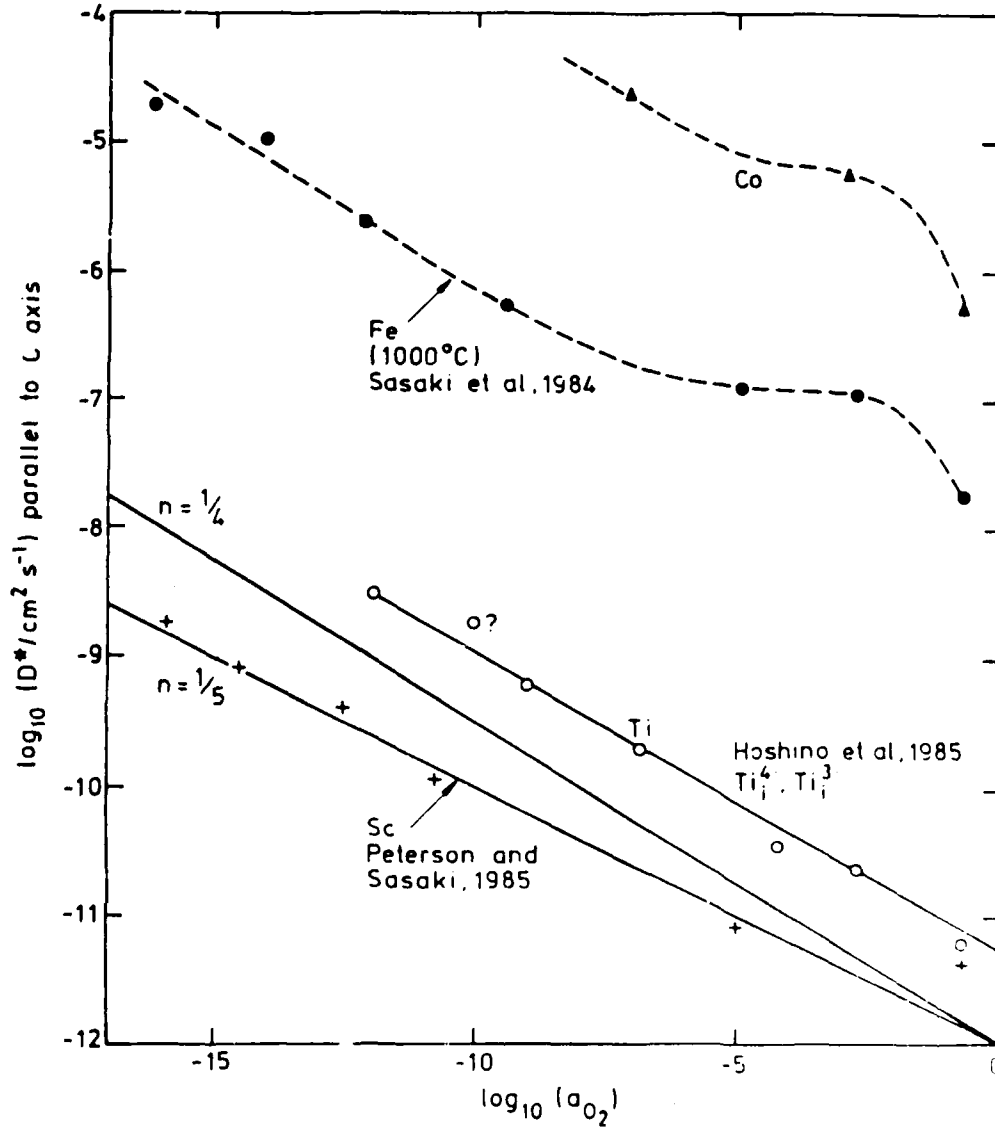
Tetragonal primitive $a = 4.59 \text{ \AA}$, $c = 2.96 \text{ \AA}$



AERE R 12405 Fig. 1

The crystal structure of TiO₂ (rutile) viewed parallel to the c axis. One of the channels containing potential interstitial sites is indicated.

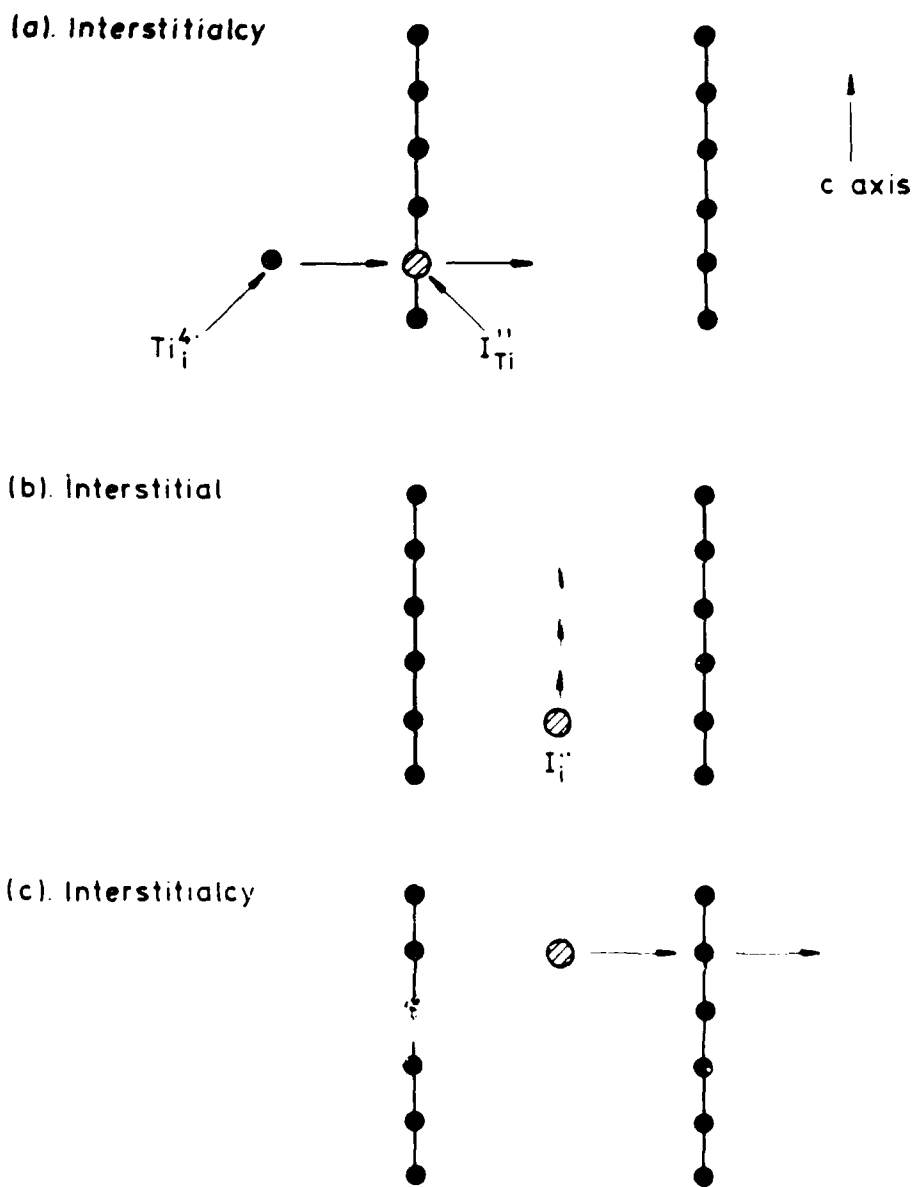
Tracer diffusion in TiO₂ at 1100°C



AERE R 12405 Fig. 2

Tracer diffusion of Co, Fe, Ti and Sc parallel to the c direction in TiO₂ as a function of a_{O_2} at 1100°C (1000°C for Fe). The indicated slopes of $n = -0.25$ and $n = -0.20$ correspond to Ti^{4+} and Ti^{3+} defects respectively (refs. 6, 12 and 13)

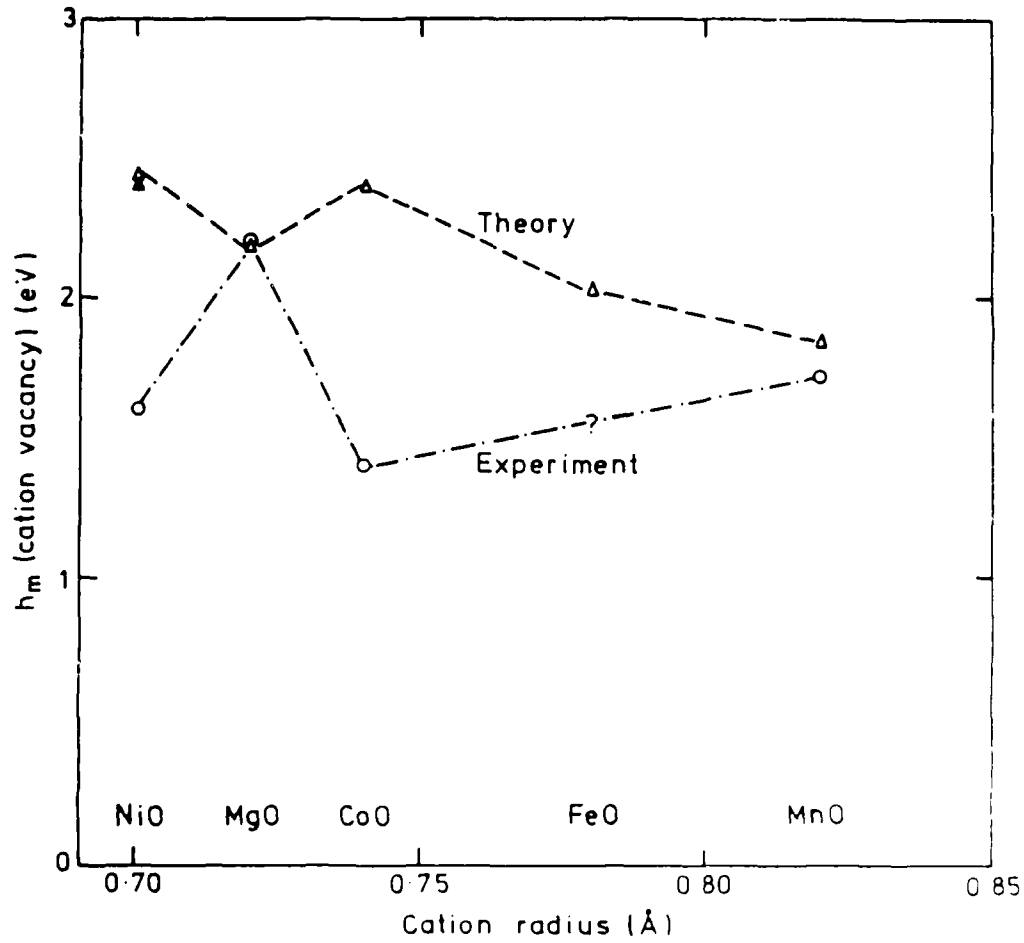
Schematic representation of impurity diffusion in TiO_2



AERE R 12405 Fig. 5

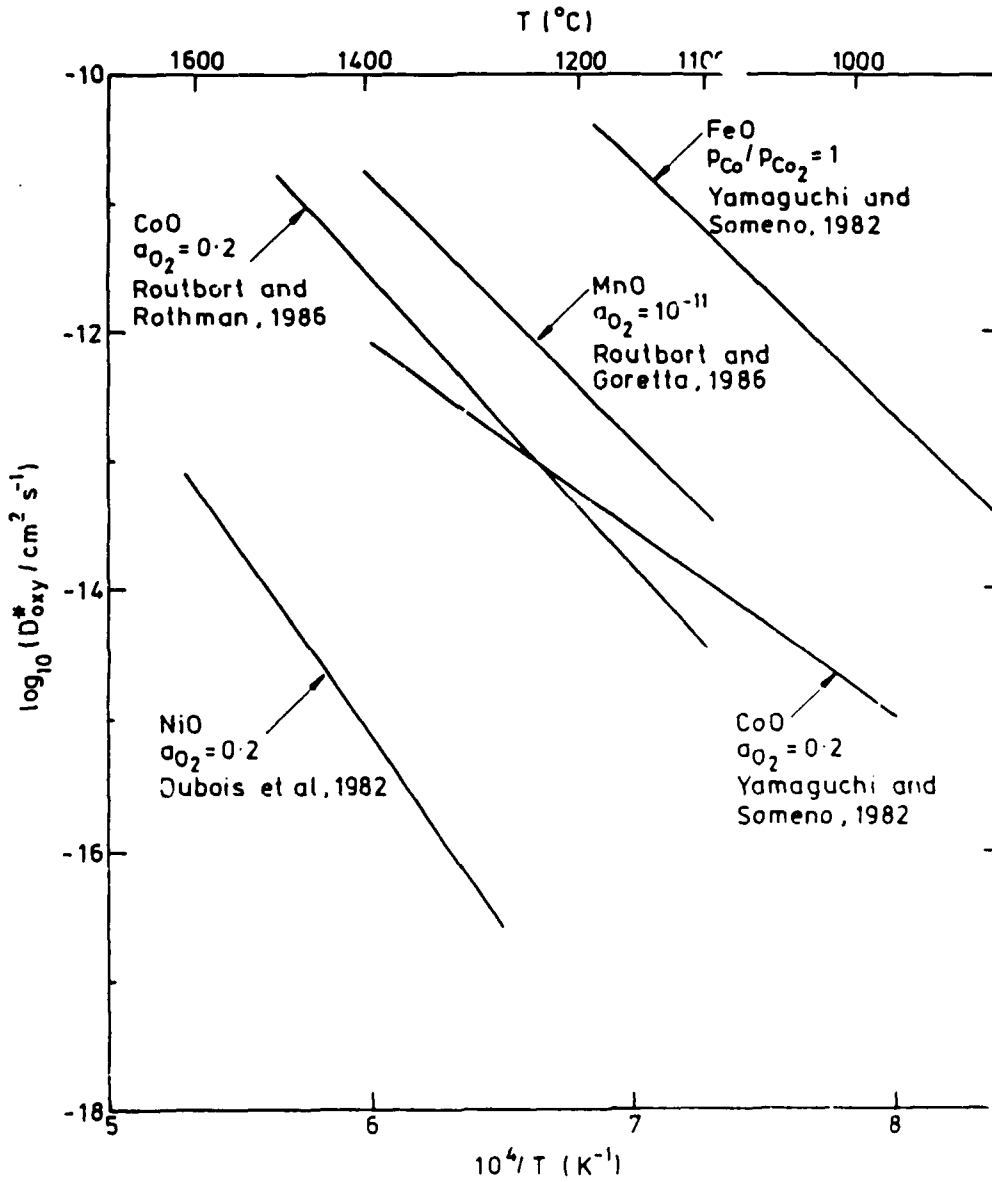
Schematic diagram indicating how fast diffusion of certain impurities along the c-direction in TiO_2 probably occurs by a mixture of interstitialcy and direct interstitial jumps

Activation energy for cation vacancy motion



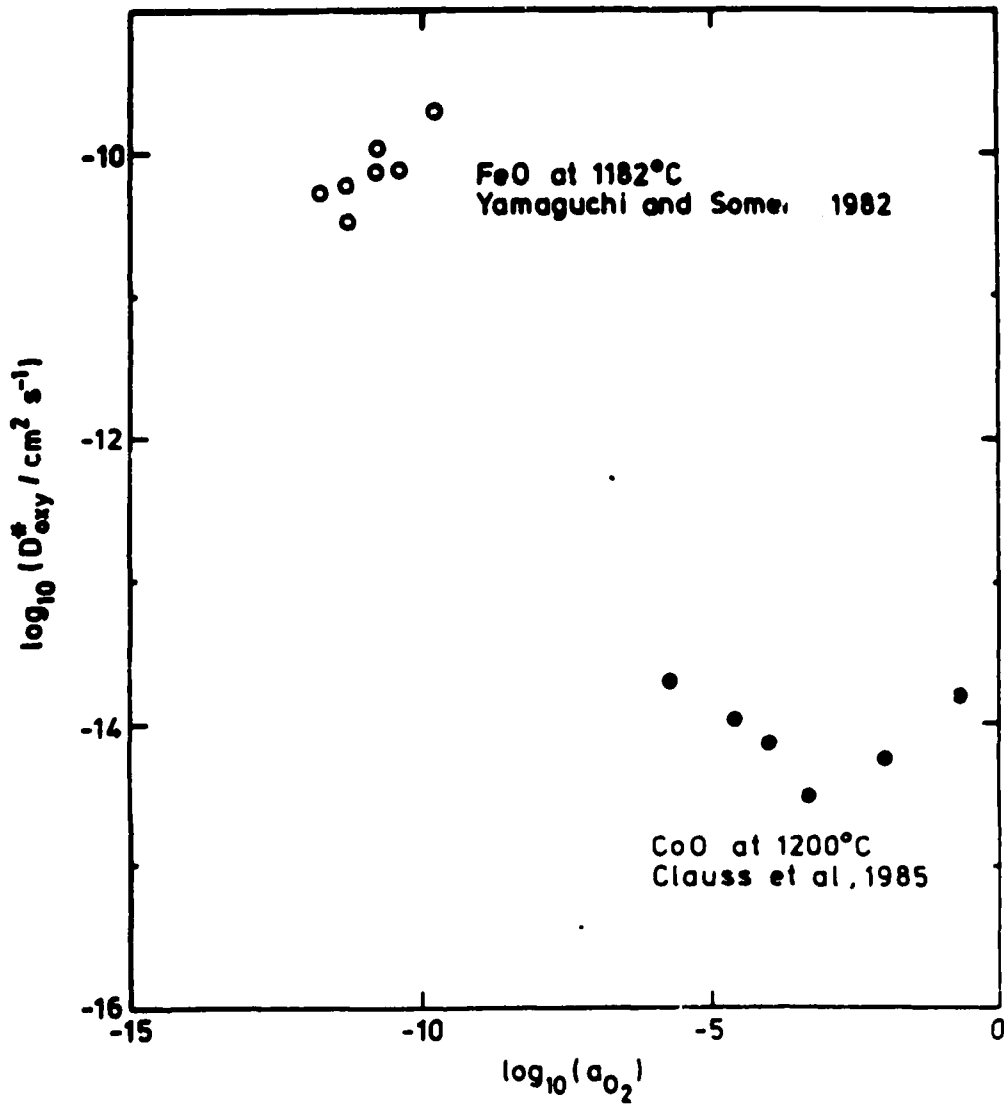
AERE R 12405 Fig. 4
Comparison between the measured and calculated enthalpies of motion for cation vacancy self diffusion in the rocksalt oxides

D_{oxy}^* in rocksalt structure oxides



AERE R 12405 Fig 5
 Arrhenius plots at constant a_{O_2} (except for FeO) of oxygen tracer self-diffusion in the rocksalt oxides
 (refs. 30-33)

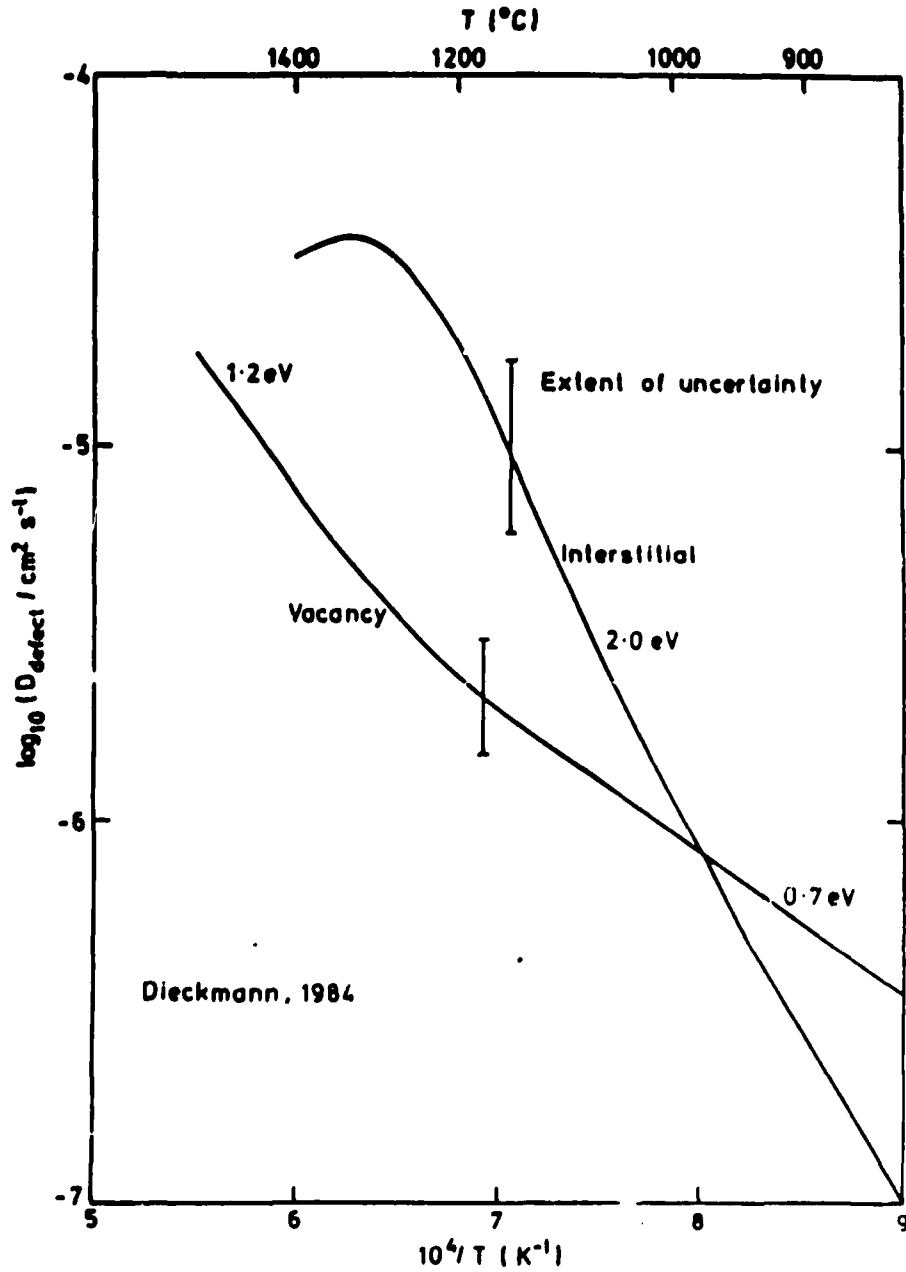
D_{oxy}^* in FeO and CoO



AERE R 12405 Fig. 6

The dependence of oxygen tracer coefficient on oxygen activity in FeO and CoO (refs. 31 and 34)

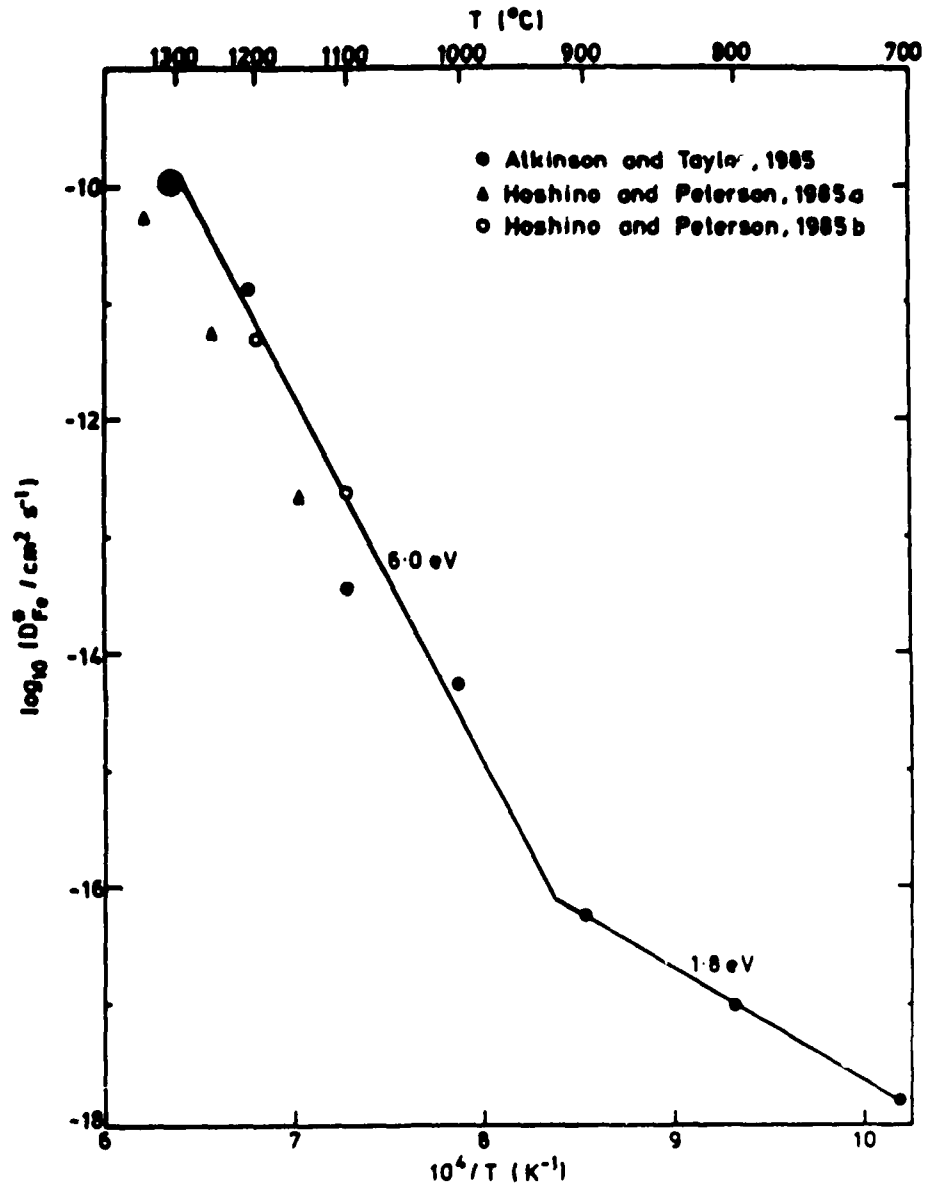
Diffusion of Fe vacancies and interstitials in Fe_3O_4



AERE R 12405 Fig. 7

Arrhenius plot of the diffusion coefficient of iron vacancies and interstitials in Fe_3O_4 . The extent of uncertainty is partly due to experiment and partly due to the range of possible correlation factors which are consistent with the experiments (ref. 24).

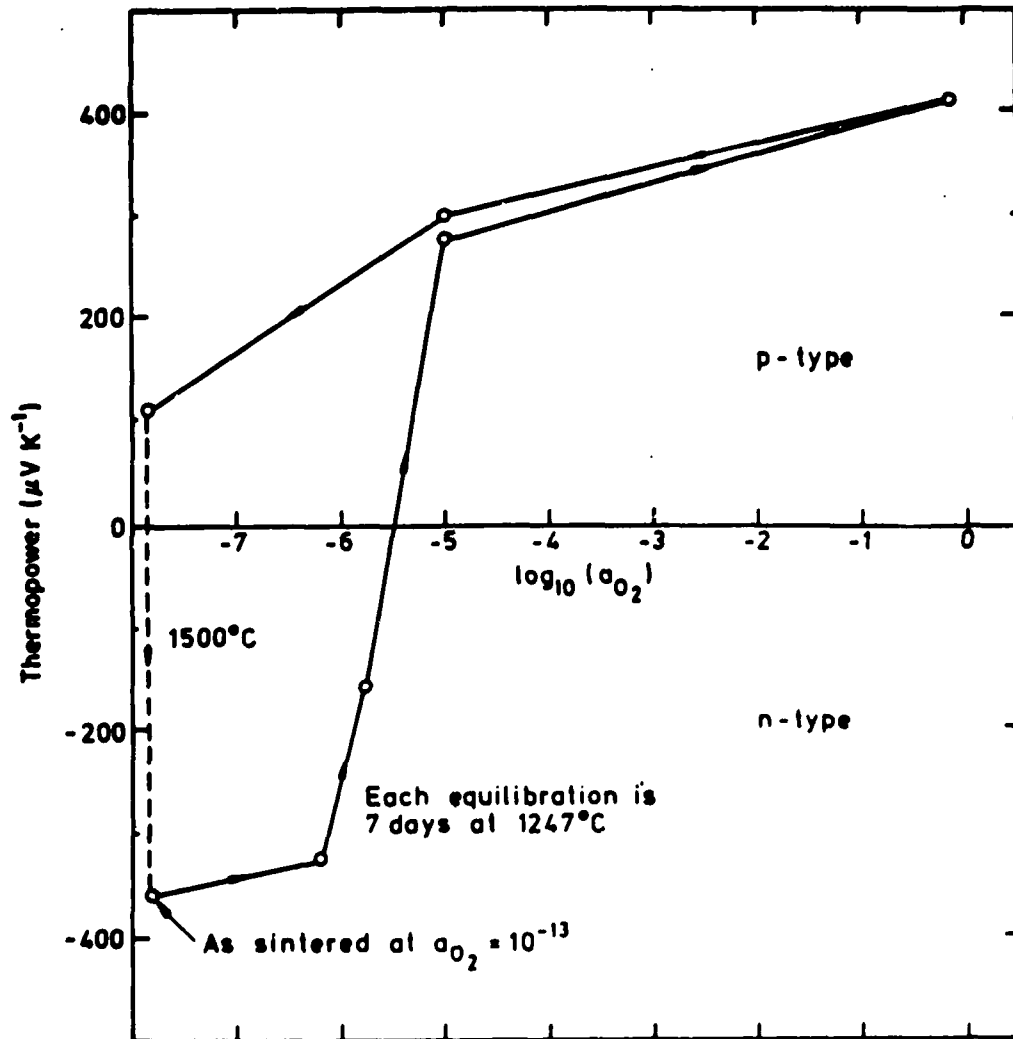
Fe in Fe₂O₃ (c-axis) at a_{O₂} = 1



AERE R 12405 Fig. 8

Arrhenius plot at constant a_{O₂} (= 1) of the tracer diffusion coefficient of Fe parallel to the c-direction in Fe₂O₃. The two data sets of Hoshino and Peterson are for crystals from different sources (refs. 51-53).

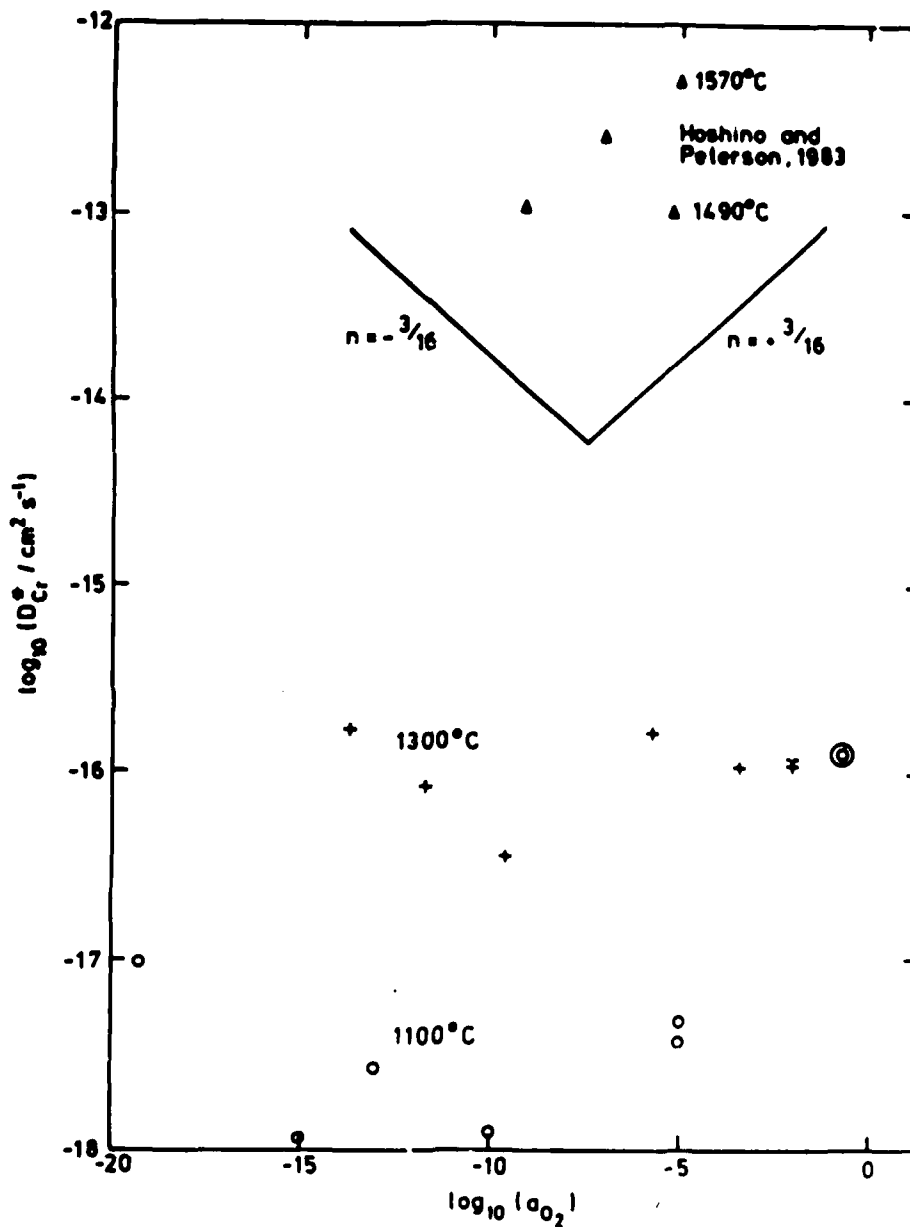
Thermoelectric power of sintered Cr_2O_3
(Young et al, 1986)



AERE R 12405 Fig. 9

The thermoelectric power of sintered Cr_2O_3 as a function of a_{O_2} . The n to p transition is complete within 7 days at 1247°C, but the reverse transition will not take place unless the temperature is raised to 1500°C (ref. 58).

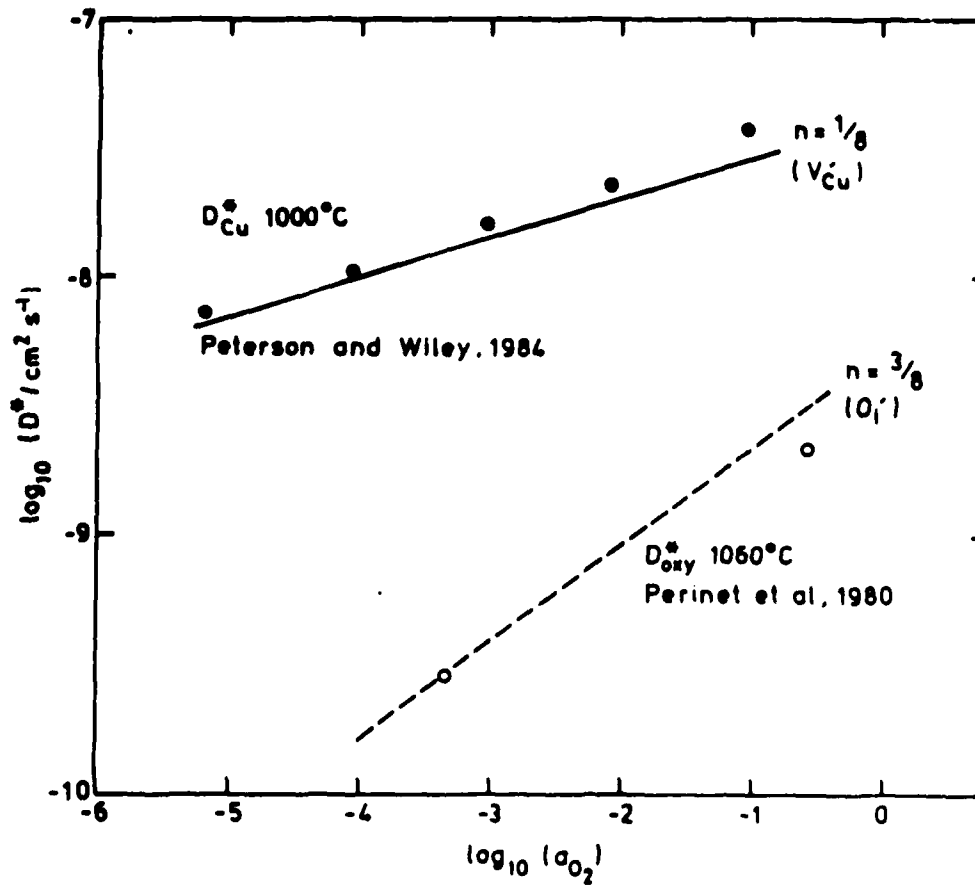
D_{Cr}^* in Cr_2O_3



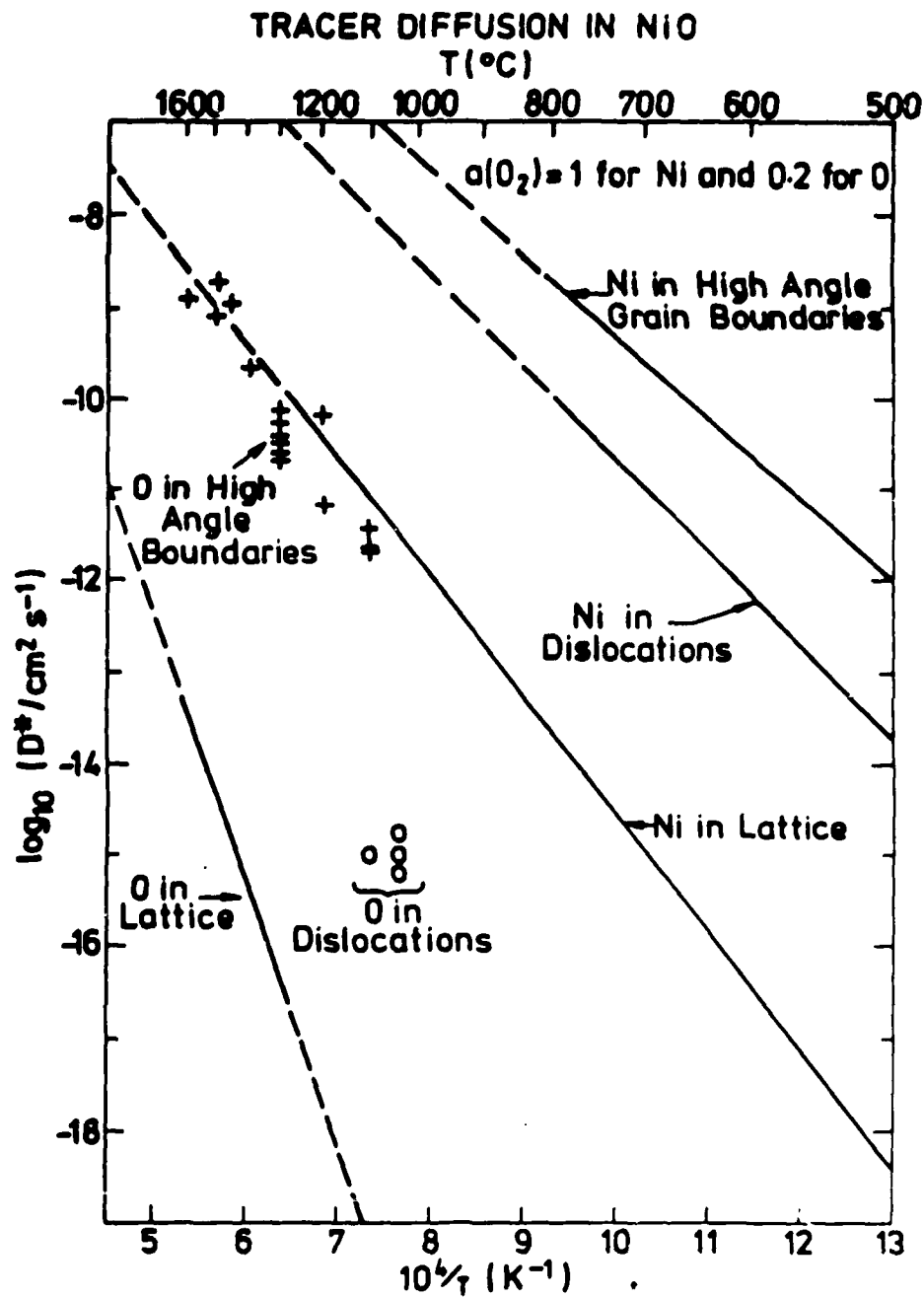
AERE R 12405 Fig. 10

Tracer diffusion of Cr parallel to the c-direction in Cr_2O_3 as a function of p_{O_2} . The indicated values of $n = +0.188$ or $n = -0.188$ are expected for diffusion by vacancies or interstitials respectively according to the simple defect model (refs. 60 and 61).

Self diffusion in Cu_2O



AERE R 12405 Fig. 11
 Tracer diffusion of Cu and oxygen in Cu_2O as a function of oxygen activity. The indicated slopes are for a simple model in which Cu diffuses by singly charged vacancies and oxygen by singly charged interstitials (refs. 62 and 63).



AERE R 12405 Fig. 12
Tracer diffusion of Ni and O in the lattice, along dislocations and along grain boundaries in NiO
 $a_{O_2} = 1$ for Ni and 0.2 for O (refs. 66, 69 and 70).